國立臺灣大學獸醫專業學院獸醫學研究所

碩士論文

Graduate Institute of Veterinary Medicine
School of Veterinary Medicine
National Taiwan University

Master Thesis

瑞氏海豚低色素沉澱疤痕之組織病理學研究

Histopathological Study on Hypopigmented Scars in Risso's Dolphins (*Grampus griseus*)

莊立亭

Li-Ting Chuang

指導教授：楊瑋誠 博士

Advisor: Wei-Cheng Yang, Ph.D.

中華民國 112 年 7 月

June, 2023

doi:10.6342/NTU202302888

國立臺灣大學碩學位論文
口試委員會審定書

瑞氏海豚低色素沉澱疤痕之組織病理學研究

Histopathological Study on Hypopigmented Scars in Risso's Dolphins (*Grampus griseus*)

本論文係莊立亭君（學號R10629012）在國立臺灣大學獸醫學系、所完成之碩士學位論文，於民國112年7月14日承下列考試委員審查通過及口試及格，特此證明

口試委員：

臺灣大學獸醫專業學院獸醫學研究所　楊瑋誠 博士 楊瑋誠

國立成功大學生命科學系　王浩文 博士 王浩文

國立嘉義大學獸醫系　詹昆衛 博士 詹昆衛

所長 張芳嘉

doi:10.6342/NTU202302888

誌謝

還記得我第一隻跟剖的海豚是小 A 送舊當晚，連夜趕去台南剖的 kogia，開到人生第一隻海豚肋骨，不知不覺就一路剖到碩二。很感謝楊瑋誠老師讓我報海豚 CC，鼓勵我念碩也放心讓我做這麼有趣的碩士題目，在我實驗遇到困難的時候不斷跟我討論找解方，即使做的很痛苦，但發現到新事物的喜悅是珍貴且難以複製的；也很感激宸儀學姊在前方開路，讓後面的皮膚人可以乘涼(?)，還悉心教導實驗室白癡的我做實驗。

真的非常感謝小 A 帶我進入這個領域，從解剖、肉眼、修片、CT…等，總是很有耐心很溫柔的教導我，一路拉拔我成長，在嘉大衝台南夜剖，然後在高速公路上看日出的經驗是我一輩子珍藏的回憶，如果沒有妳我不會走到現在；謝謝孟容帶我做實驗也帶我們喝酒；謝謝佩穎在擱淺救援時燃燒的肝跟熱情，妳滿腔的熱血跟對鯨豚的愛是我活體救援時的閃光點，讓我像嗑藥一樣撐過崩潰的救援；謝謝宜樺學姊教導我鯨豚臨床上的知識跟技術，放手讓我練習，也在我跟毓蓉手足無措的時候告訴我們方向；謝謝羅婕學姊跟三叔學長給我們很多實用的意見，讓我們可以越來越進步；也謝謝王浩文老師在台南對我的照顧，每次都關心我的摩托車，然後在解剖的時候講很多有趣的笑話跟知識，讓解剖這件事變得很有趣；謝謝紫毓學姊，在實驗方面給我很多有用的意見，妳的做圖技巧總是讓我驚艷；謝謝湘嵐跟筠婷，耐心地幫忙採皮跟解剖，來回寄了無數福馬林跟皮膚；謝謝所有四草救援中心的志工，你們讓我覺得我的青春沒有白燒。

謝謝中華鯨豚協會的養育之恩，謝謝實驗室的好夥伴，柏睿跟柏綸，跟你們去澎湖海龜健檢還有在實驗室大吵大鬧真的是很美好的回憶；謝謝我的解剖好夥伴毓蓉，真的超感激在 309 遇到妳，通宵解剖吃 sukiya 早餐、在修片室高歌杰哥不要 the 音樂劇、一起討論 case、一起搭數不清的夜車，我從妳身上學到好多，如果沒有妳我真的不知道怎麼撐下去，妳永遠都是我跟何昀的小寶貝；謝謝我上輩子的雙胞胎何昀，妳是我實驗室的浮木，在我看顯微鏡精神崩潰的時候安慰我，跟我一起開諧音梗研討會，跟我一起嘻嘻哈哈，妳讓我看到另一種活著的方式，妳讓我覺得這世界沒有我想的那麼糟，妳讓我覺得網購其實不用思考太多。謝謝 Whited 顯微鏡，雖然常常都想把你砸了，但還是拍不不少好照片。謝謝我的 J-bubu 115，雖然常常熄火，但感謝你乘載了我的青春。

doi:10.6342/NTU202302888

摘要

瑞氏海豚（*Grampus griseus*），或稱花紋海豚，因其皮膚上明顯的大量疤痕而聞名，這些疤痕通常是由海豚之間的牙齒刮傷或達摩鯊（*Isistius brasiliensis*）咬傷所造成。這些疤痕通常呈灰色至白色，使其在瑞氏海豚身上更加顯眼。瑞氏海豚的低色素沉澱疤痕具有獨特而高度重複的特徵。癒合的白色疤痕，即先前由達摩鯊咬傷所造成的深度傷口，從中心至最外層分為四部分：(1) 中央白色區域，(2) 遷移線，(3) 周圍區域，(4) 未受傷的皮膚。此為第一個針對瑞氏海豚皮膚組織學和低色素沉澱疤痕病理學方面的研究，結果顯示於瑞氏海豚的正常皮膚中，深色皮膚相較淺色皮膚擁有更多的黑色素細胞，且白色皮膚仍含有少量的黑色素細胞；於黑色素顆粒染色中亦發現深色皮膚相較淺色皮膚可見更多黑色素顆粒，且白色皮膚仍可見少量黑色素顆粒。於瑞氏海豚的低色素沉澱疤痕中未發現黑色素細胞及黑色素顆粒。此結果與先前於人類和杜洛克豬的低色素沉澱疤痕所發現的特徵不同，人類及豬的疤痕中仍可見黑色素細胞，但未見黑色素顆粒。研究結果還發現，瑞氏海豚的愈合傷口周圍存在黑色素細胞脫離的現象。此外，在網狀真皮中發現強烈的黑色素細胞抑制因子，如 Dickkopf-1。這些證據皆表明瑞氏海豚的低色素沉澱疤痕形成機制與陸地動物不同，且類似於人類白癜風患者患處的組織病理特徵。

關鍵字：海豚、瑞氏海豚、低色素沉澱疤痕、黑色素細胞喪失、黑色素細胞脫離、幹細胞因子、Dickkopf 相關蛋白 1

doi:10.6342/NTU202302888

Abstract

Risso's dolphin (*Grampus griseus*) is renowned for its prominent scarring, often resulting from tooth-rake marks during dolphin interactions or bites from cookiecutter sharks (*Isistius brasiliensis*). These scars are typically gray to white, making them conspicuous on the skin of Risso's dolphins. The hypopigmented scars in Risso's dolphins exhibit distinctive and highly repetitive characteristics. The healed white scars, which represent previously deep wounds caused by cookiecutter shark bites, can be divided into four parts from the center to the outermost layer: (1) the central white area, (2) migrating lines, (3) periphery area, and (4) the unwounded skin. This study represents the first investigation into the histology of Risso's dolphin skin and the pathology of hypopigmented scars, revealing that the darker skin regions contain a higher number of melanocytes compared to the lighter regions, while even the white skin still contains a small number of melanocytes. Additionally, darker skin areas exhibit more melanin granules than lighter skin areas, and some melanin granules are also present in the white skin areas. In the hypopigmented scars of Risso's dolphins, no melanocytes or melanin granules were observed. These findings differ from the characteristics of hypopigmented scars in human and duroc pig, where melanocytes are still present but melanin granules are absent. The study also observed melanocytes detachment in the healing wounds of Risso's dolphins. Furthermore, strong melanocyte-

doi:10.6342/NTU202302888

inhibiting factors, such as Dickkopf-1, were found in the reticular dermis. Taken together, this evidence suggests that the mechanism of hypopigmented scars in Risso's dolphins differs from that in terrestrial animals and shares similarities with the pathological features observed in human vitiligo patients.

Keywords: dolphin, Risso’s dolphin, hypopigmented scar, melanocyte loss, melanocyte detachment, SCF, DKK1

doi:10.6342/NTU202302888

Contents

doi:10.6342/NTU202302888

doi:10.6342/NTU202302888

Chapter 1 Introduction

1.1 Hypopigmented scars of Risso's dolphins

Risso's dolphins (*Grampus griseus*) are distributed across temperate and tropical oceans, and they exhibit a noticeable preference for habitats characterized by steep shelf-edges (Baird, 2009). These habitats are typically found at depths ranging from approximately 400 to 1000 meters (Azzellino et al., 2008; Baird, 2009; Canadas et al., 2002). The distribution of Risso's dolphins appears to be influenced by water temperature, as they are predominantly found in waters ranging from 15°C to 20°C, while their occurrence in waters below 10°C is rare (Baird, 2009). It is widely believed that Risso's dolphins are deep diving species which primarily rely on cephalopods as their main source of food (Blanco et al., 2006). The physical appearance of Risso's dolphins is exceptionally distinctive and conspicuous. Their head is characterized by a prominent vertical crease along the anterior surface of its melon. In most individuals, the upper jaw is devoid of teeth, while the lower jaw typically contains a limited number of teeth, ranging from 2 to 7 pairs (Baird, 2009).

The skin color patterns of Risso's dolphins undergo significant changes throughout their lifespan. Base skin appearance of infants is gray to brown, while their ventral side appears creamy-white. A distinct white anchor-shaped patch is present on the chests, along with white markings around the mouth. As infants mature, their skin color

doi:10.6342/NTU202302888

gradually darkens, often reaching near-black shades, while retaining the anchor-shaped patch on the chest. Due to the accumulation of numerous white scars, adult dolphins tend to lighten in color as they age (Baird, 2009; Bearzi et al., 2011). Older individuals can turn almost entirely white, with the exception of dorsal and pectoral fin, which remains dark in most populations. Notably, there is no reported evidence of sexual dimorphism in relation to color pattern (Bearzi et al., 2011).

Risso's dolphins are famous for their heavily scarred features, which are primarily caused by aggressive interactions with conspecifics. Scars on Risso's dolphins can also be created by marks from squid beaks or tentacles, scrapes resulting from entanglement, snake-like scars likely caused by larva migrans (Mariani et al., 2016), and deep wounds created from cookie cutter shark bites (Grace et al., 2018). These types of scars often appear white, and this characteristic can persist for a long period (Bearzi et al., 2011; Mariani et al., 2016). The white scar feature has been widely utilized for photo identification (photo-ID) (Bearzi et al., 2011; Hartman et al., 2008; Maglietta et al., 2018). Furthermore, the age estimation of Risso's dolphins has also been studied based on the accumulation of scars (Hartman et al., 2008, 2016; Mariani et al., 2016). It has been observed that adult females exhibit lower levels of scarring compared to males and are not typically observed in the whiter skin classes, suggesting that male dolphins engage in more frequent aggressive interactions with each other (Hartman et al., 2016).

doi:10.6342/NTU202302888

Another observation has shown that hypopigmented scars can disappear through repigmentation, and this phenomenon was mostly happened in immature individual (Mariani et al., 2016). This result may indicate that young individuals possess a stronger ability to restore their original skin color compared to older individuals. To date, studies on hypopigmented scars in Risso's dolphins have predominantly relied on photographic data, with no research conducted on the pathological characteristics of these scars.

1.2 Repigmentation in dolphins

Cetaceans exhibit a distinct cutaneous anatomy that is believed to represent an adaptation to their aquatic environment (Wainwright et al., 2019). The skin of dolphins is characterized by a smooth and rubbery texture, devoid of hair follicles or other skin appendages, although newborn dolphins do possess hairs on the rostrum, which are shed shortly after birth. The epidermis of dolphin skin is divided into three layers: the stratum externum, the stratum spinosum, and the stratum basale (also known as the stratum germinativum), while the stratum granulosum and the stratum lucidum are absent. In the stratum externum, most of the cells retain flattened nuclei, which is referred to as parakeratosis (Cozzi et al., 2017). Cetacean skin exhibits several remarkable features, including a thick epidermis with elongated rete ridges that intricately interdigitate with dermal ridges, also known as dermal papillae. This unique architectural arrangement is a distinguishing characteristic of cetacean skin. Moreover, the dermis of cetaceans

doi:10.6342/NTU202302888

comprises a complex network of collagen fibers, which contribute to the structural integrity and mechanical strength of the skin. Within the reticular dermis, blood vessels and nerve fibers are prominently visible (Su et al., 2023). Situated beneath the dermis is blubber, an intricately layered subcutaneous adipose tissue unique to marine mammals (Iverson, 1985). This blubber matrix comprises abundant adipocytes intricately woven with blood vessels, nerves, collagen fibers, and elastin fibers (Hashimoto et al., 2015; Reeb et al., 2007).

Several prior research studies have been dedicated to investigating melanocytes and melanin granules in the skin of cetaceans. Melanin granules are present in every layers of epidermis in cetacean skin, including the stratum corneum. The granules were positioned apically within the cells and created an "umbrella-like" structure that covered the nucleus of the keratinocytes. These traits have been reported previously for melanocytes of odontocetes and mysticetes (Martinez et al., 2011; Morales et al., 2017). Keratinocyte realignment of melanin has been described in humans and is known to constitute a protective response against UV (Menon, 2002; Rastogi et al., 2010). The extensive distribution of melanin granules was regarded as a distinctive photoprotective characteristic of cetaceans, aiding in their adaptation to aquatic life. (Morales et al., 2017).

doi:10.6342/NTU202302888

Dolphins have been reported to possess remarkable cutaneous wound healing capacity (Bossley et al, 2014; Su et al, 2022a; Elwen et al, 2010; Zasloff, 2011). There are studies have explored the histological characteristics of skin wound healing in cetaceans, specifically in bottlenose dolphins and beluga whales (Bruce-Allen & Geraci, 1985; L J. Bruce-Allen & J. R. Geraci, 1987). These studies revealed that the healing process in these species involves similar cellular and vascular changes as observed in humans and laboratory animals. Unlike terrestrial mammals, cetaceans do not form solid fibrin clots or scabs during wound healing. Instead, the wound surface in cetaceans is covered by a layer of degenerative cells interspersed with vesicles. Furthermore, some dolphin species even have the ability to restore their original skin pigmentation pattern. A recent study on Fraser's dolphins (*Lagenodelphis hosei*) demonstrated their remarkable ability to achieve complete repigmentation following full-thickness injuries (Su et al., 2022b). The study revealed that the number of melanocytes and the skin color pattern in healed wounds returned to a state similar to that of unwounded skin. Notably, during the healing process of wounds in Fraser's dolphins, melanocytes and melanin granules can be observed in the migrating tongue of the closing wound. This finding is similar to observation in migrating tongue of guinea pigs (Snell, 1963), while the situation is different from human due to the delayed recruitment of melanocytes (Heath et al., 2009). It was believed that the achievement of successful repigmentation

doi:10.6342/NTU202302888

following skin injury depends on various factors, including the migration of functional melanocytes into the neoepidermis and the synthesis as well as transfer of melanin to neighboring keratinocytes (Chadwick et al., 2013). Previous studies on Fraser's dolphins have provided valuable insights into the fundamental mechanisms underlying their repigmentation ability. However, despite sharing similar cutaneous histology characteristics, there exists a significant disparity in the appearance of scars between Fraser's dolphins and Risso's dolphins. Unlike Fraser's dolphins, the basic knowledge of skin pigmentation in Risso's dolphins are unknown, including the melanocyte number and melanin distribution in different skin colors.

1.3 Abnormal pigmentation of scars

Melanocytes are recognized as cells responsible for producing melanin, which plays vital physiological roles in photoprotection, pigmentation, and immunity. (Costin and Hearing, 2007; Gasque and Jaffar, 2015). Melanocytes produce melanin within membrane-bound organelles known as melanosomes. Subsequently, these melanosomes are transferred to the neighboring keratinocytes and positioned on the sun-exposed side of nuclei to provide protection to the epidermis against ultraviolet radiation (UVR). (Ando et al., 2012). Differences in human skin tone reflect variations in the number, size, composition and distribution of melanosomes, while melanocyte numbers generally remain relatively consistent across different ethnicity (Costin & Hearing,

doi:10.6342/NTU202302888

2007; Jennifer Y. Lin & David E. Fisher, 2007). Although normal skin pigmentation is relatively well comprehended, the mechanisms underlying both hypopigmentation and hyperpigmentation in scars remain less clear (Jennifer Y. Lin & David E. Fisher, 2007; Travis et al., 2015). Scars with abnormal pigmentation can be a serious complication for people who suffered from full thickness cutaneous injury. Deficiency of melanin in hypopigmented scars would increase the risk of UVR damage, including sunburn and skin malignancy (Shah et al., 2012). The treatment of scarring has long been an issue for plastic surgeons. Currently, there is still lack of definitive treatments for hypopigmented scar (Carney et al., 2018; Shah et al., 2012).

Several researches for hypopigmented scars have been done on Duroc pig, which are known to scar badly. Studies have demonstrated that the subsequent healing process of a full-thickness wound created on the flank of Duroc pigs results in the formation of abnormal pigmented hypertrophic scars, characterized by central hypopigmented regions surrounded by hyperpigmented regions (Carney et al., 2021; Travis et al., 2015). Regions of hypopigmented scar didn't contain melanin, while hyperpigmented scar had diffuse melanin throughout every layer of epidermis, which is similar to surrounding unwounded skin. Although macroscopic scar appearance is related to microscopic melanin deposition, the numbers of melanocytes stay approximately equal in both hyperpigmented and hypopigmented tissues (Bonnie C. Carney et al., 2019; Carney et

doi:10.6342/NTU202302888

al., 2021; Travis et al., 2015). Furthermore, hypopigmented scars have inactivated melanocytes with almost no dendrite compared to activated melanocytes with more dendrites in hyperpigmented scars (Carney et al., 2021; Shruti Dutta et al., 2020). The findings in human dyschromic hypertrophic scars are similar to those observed in Duroc pigs. A recent study on human dyschromic hypertrophic scars revealed that regions of hyperpigmentation and hypopigmentation contained the same number of melanocytes. Similar to swine, hypopigmented regions in humans were found to contain inactivated melanocytes with fewer dendrites, while hyperpigmented regions exhibited activated melanocytes with more dendrites (Carney et al., 2021).

Melanin production in melanocytes is a complex process that is regulated by multiple extrinsic factors. Several extracellular signals are transduced through dedicated signaling pathways, which ultimately converge on microphthalmia-associated transcription factor (MITF). MITF is a transcription factor involved in various mechanisms that modulate melanogenesis (Serre et al., 2018). Upon damage to keratinocytes caused by UVR, the tumor protein 53 (p53) is upregulated (Jennifer Y. Lin & David E. Fisher, 2007). Subsequently, p53 acts as a transcription factor, promoting the upregulation of pro-opiomelanocortin (POMC), the precursor of adrenocorticotropic hormone (ACTH) and α-melanocyte stimulating hormone (α-MSH). ACTH and α-MSH then bind to the melanocortin 1 receptor (MC1R) present on melanocytes, eventually

doi:10.6342/NTU202302888

leading to the transcription of MITF (Jennifer Y. Lin & David E. Fisher, 2007; Serre et al., 2018). Concurrently, stem cell factor (SCF), a growth factor secreted by keratinocytes and fibroblast, binds to melanocyte stem cell factor receptor (cKIT) (Cichorek et al., 2013; Serre et al., 2018). This ligand-receptor interaction activates several pathways, including AKT and MAP kinase pathways. These kinase cascades phosphorylate MITF, resulting in the stimulation of melanogenesis (Jennifer Y. Lin and David E. Fisher, 2007; Park et al., 2009; Serre et al., 2018). In the study of Duroc pig, the melanogenesis of hypertrophic scars does not follow the conventional mechanism involving the p53 pathway induced by UV-light exposure. Instead, it proceeds through a distinct pathway specific to hypertrophic scars. In comparison to the hyperpigmented regions, hypopigmented regions exhibit reduced levels of certain factors, such as POMC, ACTH, α-MSH, SCF, as well as receptors including c-KIT and MC1R (Carney et al., 2019). However, the regulation of melanocytes in scars and the exact mechanism behind abnormal pigmented scar are not yet fully understood.

Interestingly, the hypopigmented scars in terrestrial animals and marine mammals appear quite similar in appearance, despite the significant differences in their skin architecture features. The factors contributing to this divergence remain unclear and require further investigation. However, our current understanding regarding the basic histopathological characteristics of white scars in Risso's dolphins remains unknown.

doi:10.6342/NTU202302888

This study focused on extracellular factor such as stem cell factor and Dickkopf-1. Stem cell factor (SCF), also known as Kit ligand (KITLG) or mast cell growth factor, is produced in various cell types in the skin, such as keratinocytes, fibroblasts, and endothelial cells (Grabbe et al., 1994). The receptor for SCF, c-KIT, is expressed on the surface of melanocytes (Grichnik et al., 1998). Several studies have demonstrated that SCF plays a critical role in the development, differentiation, proliferation, and melanogenesis of melanocytes (Li et al., 2018). Dickkopf-1 (DKK1) is a secreted antagonist of the canonical Wnt signaling pathway, which interacts with the Wnt receptor lipoprotein receptor-related protein 6 (LRP6) (Yamaguchi et al., 2007). DKK1 inhibits the melanogenesis and proliferation of melanocytes (Yamaguchi et al., 2007, 2008). The aim of this study including investigates the migration of melanocytes, the regulation of melanin production, and the factors governing melanocytes proliferation and migration in hypopigmented scars of Risso's dolphins.

doi:10.6342/NTU202302888

Chapter 2 Materials and methods

2.1 Sample collection and preparation

Skin samples were obtained from five deceased stranded Risso's dolphins in Taiwan, as elaborated in Table 1. All procedures involving animals were conducted under the authorization of the Ocean Conservation Administration (OCA), Taiwan (Permit #120004572). The evaluation of body condition and carcass condition was conducted following methodologies established in earlier research (Melissa et al., 2014). The samples included normal skin and full-thickness wounds created by cookie cutter shark (*Isistius brasiliensis*) bites. Dark skin samples were collected from dorsal-lateral, dark-gray skin samples from lateral trunk, light-gray skin samples from peduncle, grayish withe samples from thorax and white skin samples from ventral side. The sampling locations (N1-10) in the current study are shown in Figure 1. Full-thickness wounds were categorized into stages 1 to 5, as outlined in a previous study. (Figure 2,3) (Su et al., 2022a). The sampling locations within the hypopigmented scars are shown in Figure 4. Tissues were fixed in 10% neutral buffered formalin for a period of 3 days, followed by embedding in paraffin.

2.2 Fontana-Masson staining

Skin samples were sectioned into 4 μm slices for Fontana-Masson staining. The slides underwent deparaffinization using xylene, followed by gradual rehydration

doi:10.6342/NTU202302888

through a series of ethanol solutions. Subsequently, Fontana-Masson staining was performed according to established protocols. Photomicrographs were acquired utilizing a Whited WM100 microscope (Whited, Taiwan).

2.3 Immunohistochemical staining

The skin tissues were sliced into 7 μm slices for immunohistochemical (IHC) staining. These sections were then baked at 60°C for one hour, followed by deparaffinization and rehydration. Antigen retrieval was carried out using Uni-trieve (Innovex Biosciences, Richmond, CA, USA) overnight at 40°C. For IHC study, the Super sensitive™ polymer-HRP detection system (BioGenex Laboratories Inc., Los Angeles, CA, USA) was utilized. The sections were rinsed in TBST (Tris-buffered saline with 0.1% Tween® 20 Detergent) after each step. In order to block non-specific binding, the sections were treated with Power Block™ universal blocking reagent (BioGenex Laboratories Inc., Los Angeles, CA, USA) for 10 minutes at room temperature. The slides were incubated overnight with cocktail primary antibodies (ab733, Abcam, Cambridge, UK, diluted 1:50) in Power Block™ at 4°C. After the overnight incubation, the sections were subjected to a 20 minute exposure to 1% methanol peroxide at room temperature. Subsequently, the Super enhancer™ reagent was applied for 30 minutes at room temperature, followed by the application of Polymer HRP reagent for 1 hour at room temperature. Next, the sections were incubated with a

doi:10.6342/NTU202302888

3-amino-9-ethylcarbazole (AEC) substrate solution at room temperature for 7 minutes. Counterstaining was performed using Mayer's hematoxylin for 20 seconds. Finally, the sections were mounted with aqueous mounting media. Photomicrographs were acquired utilizing a Whited WM100 microscope (Whited, Taiwan).

2.4 Melanocytes counting

Immunohistochemical (IHC) staining was conducted using a cocktail antibody (ab733, Abcam, Cambridge, UK, diluted 1:50) to assess melanocyte count. Cells exhibiting positive staining were manually enumerated along the basement membrane within a ×500 viewing field. The extent of the basement membrane examined ranged from 15 to 200 mm, contingent upon wound dimensions and skin coloration patterns. The findings are presented as the number of melanocytes per millimeter.

2.5 Immunofluorescence staining

Skin tissues were sectioned into 7 μm slices for immunofluorescence (IF) staining. Sections were baked at 60°C for one hour. Deparaffinization was carried out using xylene, followed by rehydration through graded ethanol. Between each subsequent step, the sections were rinsed in TBST (Tris-buffered saline with 0.1% Tween®20 Detergent) for 5 minutes, repeated 2-3 times. Antigen retrieval was performed overnight at 40°C using Uni-trieve (Innovex Biosciences, Richmond, CA, USA). The primary antibodies used in this study were as follows: anti-SCF antibody (ab64677, rabbit polyclonal,

doi:10.6342/NTU202302888

Abcam, Cambridge, UK, diluted 1:500 in blocking buffer) and anti-DKK1 antibody (EPR4759, rabbit monoclonal, Abcam, Cambridge, UK, diluted 1:300 in blocking buffer). The sections were incubated in blocking buffer at room temperature for 1 hour, followed by overnight incubation at 4°C with primary antibodies. Negative control slides were incubated with PBS only. After overnight incubation, sections were incubated with 1% methanol peroxide at 4°C for 30 minutes, and then with the secondary antibody, Alexa Fluor^{TM}594 goat-anti-rabbit IgG (A11012, Invitrogen, diluted 1:200), at room temperature for 1.5 hours. Nuclei were counterstained with Hoechst 33342 dye (H3570, Invitrogen, diluted 1:1000) for 5 minutes, and slides were then mounted with aqueous mounting media. Images were captured using an Olympus IX83 epifluorescence microscope (Olympus, Tokyo, Japan).

doi:10.6342/NTU202302888

Chapter 3 Result

3.1 Normal skin

3.1.1 Fontana-Masson staining in normal skin

Melanin staining was visualized through Fontana-Masson staining in skin samples categorized as dark, dark-gray, light-gray, and white. A higher quantity of melanin granules was discernible in darker skin compared to lighter skin. However, the intensity of melanin staining was not quantified. Across all skin samples utilized in this study, melanin granules were observed throughout the epidermal layers, including the stratum basale, stratum spinosum, and stratum externum. These melanin granules were positioned on the apical side of cell nuclei, serving to shield the nucleus from ultraviolet (UV) radiation. (Figure 5).

3.1.2 Melanocytes count in normal skin

The quantities of melanocytes differed across skin of varying colors, with the greatest number observed in dark skin (12.7-18.2), followed by dark-gray skin (9.3-12), light-gray skin (5.5-6.4), and the lowest number of melanocytes in white skin (0.15-0.52) (Table 2). The distribution of melanocytes was primarily concentrated at the bottom of the rete ridge. The morphology of melanocytes exhibited a round to oval shape or a dendritic shape with long cytoplasmic processes (Figure 6).

doi:10.6342/NTU202302888

3.1.3 Immunofluorescence (IF) staining in normal skin

3.1.3.1 Signal distribution of SCF in normal skin

The distribution of the melanocyte growth factor, SCF, was examined in normal skin using immunofluorescence staining. SCF signals could be observed in the cytoplasm of keratinocyte, fibroblast and endothelial cell. Distribution of SCF in Risso's dolphins was strong and positive in almost every layer of epidermis, and were more pronounced especially in basal layer (Figure 7D-E). Signals were absent in the stratum corneum. In reticular dermis, weak signals could be found in cytoplasm of fibroblast (Figure 7F-G). Intestine tissue of Risso's dolphin was used as positive control for SCF antibody by immunohistochemical staining (Figure 7H). This distribution pattern was constant in normal skin, despite different skin colors (Figure 8).

3.1.3.2 Signal distribution of DKK1 in normal skin

The distribution of the melanocyte inhibitor, DKK1, was examined in normal skin using immunofluorescence staining. DKK1 signals could be observed in the cytoplasm and nucleus of keratinocyte and fibroblast. Distribution of DKK1 in Risso's dolphin was strong and positive in almost every layer of epidermis, and were more pronounced especially in basal layer (Figure 9D-E). Signals were absent in the stratum corneum. In reticular dermis, weak signals could be found in cytoplasm of fibroblast (Figure 9F-G). Liver tissue of Risso's dolphin was used as positive control for DKK1 antibody by

doi:10.6342/NTU202302888

immunohistochemical staining (Figure 9H). This distribution pattern was constant in normal skin, despite different skin color (Figure 10).

3.2 Wounds

3.2.1 Gross appearance of hypopigmented scars

The hypopigmented scars of Risso's dolphins exhibited different gross characteristics throughout the healing process: Stage 1 wounds, new wounds; Stage 2 wounds, wounds in the initial healing stage with no granulation. There was no difference in skin color between edge of stage 2 wounds and surrounding unwounded skin (Figure 2A); Early stage 3 wounds, the ratio of the diameter of the initial wound to the minor axis of the incompletely epithelialized granulation tissue was greater than one-half. The newly grown skin appeared uniformly grayish-white in color (Figure 2E); Middle stage 3 wounds, the ratio of the diameter of the initial wound to the minor axis of the incompletely epithelialized granulation tissue was lower than one-half. Peripheral areas and migrating lines have become visible in the re-epithelialized skin (Figure 2F); Late stage 3 wounds, incompletely epithelialized wound and granulation tissue is no longer visible to the naked eye. Central white areas had emerged in the re-epithelialized skin (Figure 2G); Stage 4 wounds, healed wound with vascular and cellular blubber. Central white areas, migrating lines and peripheral areas can be clearly seen in the scars (Figure 2C); Stage 5 wounds, healed wound without vascular and cellular blubber.

doi:10.6342/NTU202302888

Pigmentation feature was similar to stage 4 wounds (Figure 2D).

3.2.2 Fontana-Masson Staining in wounds

In early stage 3 wounds, melanin granules were observed in every layer of the neoepidermis, including the tip of the migrating tongue (Figure 11). However, in stage 4 and 5 wounds, the central white areas showed an absence of melanin granules throughout the epidermis. Additionally, a substantial amount of melanin granules could be observed in the epidermis of the migrating lines, and a certain amount of melanin granules were also present in the peripheral areas through the epidermis (Figure 12).

3.2.3 Melanocytes count in wounds

In early stage 3 wounds, the number of melanocytes ranged from 1.52 to 4.02 in the basal layer of the migrating tongue. However, in the late stage 3 wound, no melanocytes were observed in the basal layer of the central white areas. Meanwhile, the number of melanocytes ranged from 2.85 to 4.59 in the basal layer of the migrating lines and periphery areas. In stage 4 and 5 wounds, no melanocytes were present in the central white areas. The dark migrating lines contained 10.72 to 12.03 melanocytes, while the grayish white migrating lines had 3.35 to 3.5 melanocytes. The light-gray peripheral areas had 9.59 to 10.5 melanocytes, while the grayish white peripheral areas had 4.13 to 12.79 melanocytes (Table 3).

doi:10.6342/NTU202302888

3.2.4 Immunofluorescence (IF) staining in wounds

3.2.4.1 Melanocytes detachment

In the periphery of the migrating tongue in early stage 3 wounds, several cocktail-positive melanocytes were observed in the suprabasal layer of the epidermis, including the stratum spinosum and at the border between the stratum spinosum and stratum externum. The detached melanocytes exhibited an oval or round morphology, and no melanocytes with dendrites were observed in suprabasal layer (Figure 13). The phenomenon of melanocytes detachment was observed exclusively at the periphery of stage 3 wounds in 3-5 stages wounds samples.

4.2 Signal distribution of SCF in wounds

The distribution of the melanocyte growth factor, SCF, was examined in different stages of wounds using immunofluorescence staining. In early stage 3 wounds, SCF exhibited a pronounced and strong distribution in the migrating tongue and cytoplasm of fibroblasts in the reticular dermis (Figure 14). However, in the late stage 3 wound, SCF signals were weak in both the epidermis and reticular dermis of the central white area (Figure 15). In stages 4-5 wounds, SCF signals were positive in the epidermis, while weak signals could be found in the cytoplasm of fibroblasts in central white areas (Figure 16,17). The distribution pattern of SCF in stages 4-5 wounds was similar to that of normal skin.

doi:10.6342/NTU202302888

4.3 Signal distribution of DKK1 in wounds

The distribution of the melanocyte inhibitor factor, DKK1, was examined in different stages of wounds using immunofluorescence staining. In early stage 3 wounds, DKK1 exhibited a positive and strong distribution in the migrating tongue and cytoplasm of fibroblasts in the reticular dermis (Figure 18). In the central white areas of the late stage 3 wound, DKK1 signals were positive in the migrating tongue and particularly strong in fibroblasts of the reticular dermis (Figure 19). In stages 4-5 wounds, DKK1 signals were positive in the epidermis, while weak signals could be observed in the cytoplasm of fibroblasts in central white areas (Figure 20,21). The distribution pattern of DKK1 in stages 4-5 wounds was similar to that of normal skin.

doi:10.6342/NTU202302888

Chapter 4 Discussion

This is the first study, to our knowledge, that focused on the histology of skin pigmentation and the pathology of hypopigmented scars in Risso's dolphins. In the normal skin of Risso's dolphins, darker skin typically has a higher number of melanocytes compared to lighter skin. Furthermore, melanin granules were observed in every layer of the epidermis, with a greater amount of melanin observed in darker skin compared to lighter skin. The results of melanocytes counting and melanin staining are similar to the findings in normal skin of Fraser's dolphins (Su et al., 2022b). Present study revealed the absence of melanocyte and melanin staining in healed hypopigmented scars of Risso's dolphins, which differs from unwounded white skin containing a few melanocytes and melanin granules. In comparison to other species, previous research in humans and Duroc pigs showed that hypopigmented scars still contain a significant number of melanocytes (Carney et al., 2021). However, these melanocytes did not produce melanin in the hypopigmented region of human and pigs. In white scars of Fraser's dolphins, melanocytes were found to be able to restore to approximately the same number as those in unwounded white skin (Su et al., 2022b). Furthermore, the melanocytes observed in white scars of Fraser's dolphins demonstrated the ability to produce melanin, which is similar to the situation observed in unwounded white skin. In conclusion, the results indicate that the mechanisms underlying

doi:10.6342/NTU202302888

hypopigmented scars may vary between species. Terrestrial animals such as humans and pigs lack the ability for melanogenesis in hypopigmented scars. In contrast, Fraser's dolphins have the ability to recover melanocyte function similar to normal skin. However, in the case of Risso's dolphins, it is possible that either melanocytes are absent or undergo significant loss during the wound healing process, resulting in the observed hypopigmented scars.

The time point of melanocyte recruitment in wounds can vary among different species (Table 4 and Figure 22). In human studies, it has been observed that melanocytes were absent in the migrating tongue (Heath et al., 2009). Additionally, a delay in the recruitment of melanocytes was observed after complete re-epithelization (Breathnach, 1960). In contrast, Fraser's dolphins exhibited functional melanocytes in the migrating tongue of healing wounds as well as in mature white scars (Su, Wang, et al., 2022b). In order to gain a better understanding in survival of melanocytes through the healing process in Risso's dolphins, melanocytes counting in different stages of wounds was performed. Based on the result, it was observed that there were a certain number of melanocytes presented in the migrating tongue of early stage 3 wounds. However, no melanocytes were found in the late stage 3 migrating tongue. Furthermore, the absence of melanocytes persisted in the center white region of stage 4 and 5 wounds. This suggests that melanocytes were not absent at the beginning of wound healing, but

doi:10.6342/NTU202302888

rather underwent a decrease in number as the wound progressed through the re-epithelization phase in Risso's dolphin.

Previous studies on the mechanism of melanocyte loss have primarily focused on human patients with vitiligo. Vitiligo, which is the most common chronic acquired depigmenting disorder, is characterized by the loss of melanocytes from the basal layer of the epidermis (Ezzedine et al., 2012). The pathogenesis of vitiligo is believed to be multifactorial and involves autoimmune factors, as well as oxidative stress (Dammak et al., 2009) and mechanical stress (Gauthier et al., 2003; Wagner et al., 2015). In vitiligo patients, a study has highlighted the absence or discontinuous distribution of cell-cell adhesion proteins, such as E-cadherin (Ecad), which play a role in regulating the interaction between keratinocytes and melanocytes (Wagner et al., 2015). Additionally, it has been reported that melanocytes can detach and undergo transepidermal elimination in non-lesional vitiligo skin when subjected to minor mechanical pressure (Gauthier et al., 2003). These detached melanocytes can be found in suprabasal locations, including the stratum spinosum, stratum granulosum, as well as within and outside the stratum corneum. Interestingly, similar melanocyte detachment was also observed in the hypopigmented scars of Risso's dolphins. This result indicated that wound healing of Risso's dolphins may experience alteration of cell-cell adhesion.

doi:10.6342/NTU202302888

Furthermore, mechanical pressure may be one of the precipitating factors causing detachment of melanocytes. The wounds may experience mechanical pressure or trauma such as water pressure, as well as friction generated during animal swimming. Additionally, swollen wounds could disrupt the streamlined body shape of the animal, potentially causing increased friction. Alteration of melanocyte-keratinocyte adhesion and mechanical pressure together may contribute as potential factors leading to the detachment and loss of melanocytes in Risso's dolphin. Further studies should be conducted to investigate adhesion markers such as E-cadherin in order to clarify the melanocyte-keratinocyte adhesion in Risso's dolphins.

In addition to mechanical pressure, extracellular factors play a crucial role in the survival, migration, proliferation, differentiation, and melanogenesis of melanocytes. This study specifically focused on growth factors such as stem cell factor (SCF) and inhibitors like Dickkopf-1 (DKK1). The SCF/KIT signaling pathway is widely recognized as a key pathway in melanogenesis(Serre et al., 2018). In the previous study of Duroc pigs, the hypopigmented regions displayed reduced levels of SCF compared to the hyperpigmented regions (Carney et al., 2019). Furthermore, besides its function in melanocytes, SCF is also essential for wound closure as it promotes the recruitment and migration of keratinocytes and fibroblasts (Wang et al., 2020). However, the distribution pattern of SCF in Risso's dolphins did not correspond to the actual pigmentation. Strong

doi:10.6342/NTU202302888

SCF signals were observed in the migrating tongue of early stage 3 wounds and in the central white region of stage 4-5 wounds, even though there were either no melanocytes or only a few present. This discrepancy suggests that SCF may not have the ability to maintain the normal function of melanocytes in these specific wound areas.

DKK1 exhibits high expression levels in palmoplantar fibroblasts and contributes to the thickening and hypopigmentation of the palmoplantar epidermis (Yamaguchi et al., 2004, 2008). DKK1 inhibit the function and proliferation of melanocytes(Rani et al., 2018). Additionally, DKK1 inhibits melanin uptake and promotes the proliferation of keratinocytes (Yamaguchi et al., 2008). DKK1 is also highly expressed in the dermis of vitiligo lesion (Esmat et al., 2018; Keswell et al., 2012). In results of Risso's dolphin, DKK1 signals were strong in the cytoplasm of fibroblast in early and late stage 3 wounds. It provided a potential explanation for the loss of melanocytes observed through early and late stage 3 wounds. Moreover, the presence of DKK1 in the dermis and melanocyte detachment may suggest the involvement of a vitiligo-like pathway in Risso's dolphins. However, it should be noted that the expression pattern of melanocyte factors may not correspond to the actual pigmentation phenotype. Furthermore, without the presence of specific receptors on melanocytes, such as SCF/Kit and DKK1/LRP6, the activation of melanocytes will not be influenced even in the presence of high concentrations of cytokines. Future research in this study should conduct more

doi:10.6342/NTU202302888

quantitative investigations on melanocyte receptors to clarify the actual effects of melanocyte factors on melanocytes themselves.

doi:10.6342/NTU202302888

Reference:

1. Ando, H., Niki, Y., Ito, M., Akiyama, K., Matsui, M. S., Yarosh, D. B., & Ichihashi, M. (2012). Melanosomes are transferred from melanocytes to keratinocytes through the processes of packaging, release, uptake, and dispersion. *Journal of Investigative Dermatology*, *132*(4), 1222–1229. https://doi.org/10.1038/jid.2011.413
2. Azzellino, A., Gaspari, S., Airoldi, S., & Nani, B. (2008). Habitat use and preferences of cetaceans along the continental slope and the adjacent pelagic waters in the western Ligurian Sea. *Deep-Sea Research Part I: Oceanographic Research Papers*, *55*(3), 296–323. https://doi.org/10.1016/j.dsr.2007.11.006
3. Baird, R. W. (2009). Risso's Dolphin: Grampus griseus. In *Encyclopedia of marine mammals* (pp. 975–976).
4. Bearzi, G., Reeves, R. R., Remonato, E., Pierantonio, N., & Airoldi, S. (2011). Risso's dolphin Grampus griseus in the Mediterranean Sea. In *Mammalian Biology* (Vol. 76, Issue 4, pp. 385–400). https://doi.org/10.1016/j.mambio.2010.06.003
5. Blanco, C., Raduán, M. Á., & Raga, J. A. (2006). Diet of Risso's dolphin (Grampus griseus) in the western Mediterranean Sea. *Scientia Marina*, *70*(3), 407–411.
6. Bonnie C. Carney, Jason H. Chen, Jenna N. Luker, Abdulnaser Alkhali, Daniel Y. Jo, Taryn E. Travis, Lauren T. Moffatt, Cynthia M. Simbulan-Rosentha, Dean S. Rosentha, & Jeffrey W. Shupp. (2019). Pigmentation diathesis of hypertrophic scar: An examination of known signaling pathways to elucidate the molecular pathophysiology of injury-related dyschromia. *Journal of Burn Care and Research*, *40*(1), 58–71. https://doi.org/10.1093/jbcr/iry045
7. Breathnach, A. S. (1960). Melanocytes in early regenerated human epidermis. *Journal of Investigative Dermatology*, *35*(4), 245–251.
8. Bruce-Allen, L., & Geraci, J. R. (1985). Wound Healing in the Bottlenose Dolphin Tursiops fruncafus. *Canadian Journal of Fisheries and Aquatic Sciences* , *42*(2), 216–228. www.nrcresearchpress.com
9. Canadas, A., Sagarminaga, R., & Garcia-Tiscar, S. (2002). Cetacean distribution related with depth and slope in the Mediterranean waters off southern Spain. *Deep-Sea Research I*, *49*, 2053–2073.
10. Carney, B. C., McKesey, J. P., Rosenthal, D. S., & Shupp, J. W. (2018). Treatment strategies for hypopigmentation in the context of burn hypertrophic scars. *Plastic and Reconstructive Surgery - Global Open*, *6*(1). https://doi.org/10.1097/GOX.0000000000001642
11. Carney, B. C., Travis, T. E., Moffatt, L. T., Johnson, L. S., McLawhorn, M. M., Simbulan-Rosenthal, C. M., Rosenthal, D. S., & Shupp, J. W. (2021).

doi:10.6342/NTU202302888

Hypopigmented burn hypertrophic scar contains melanocytes that can be signaled to re-pigment by synthetic alpha-melanocyte stimulating hormone in vitro. *PLoS ONE*, *16*(3 March). https://doi.org/10.1371/journal.pone.0248985

12. Chadwick, S. L., Yip, C., Ferguson, M. W. J., & Shah, M. (2013). Repigmentation of cutaneous scars depends on original wound type. *Journal of Anatomy*, *223*(1), 74–82. https://doi.org/10.1111/joa.12052
13. Cichorek, M., Wachulska, M., Stasiewicz, A., & Tymińska, A. (2013). Skin melanocytes: Biology and development. *Postepy Dermatologii i Alergologii*, *30*(1), 30–41. https://doi.org/10.5114/pdia.2013.33376
14. Costin, G.-E., & Hearing, V. J. (2007). Human skin pigmentation: melanocytes modulate skin color in response to stress. *The FASEB Journal*, *21*(4), 976–994. https://doi.org/10.1096/fj.06-6649rev
15. Cozzi, B., Huggenberger, S., & Oelschläger, H. (2017). *Anatomy of Dolphins: Insights into Body Structure and Function*.
16. Dammak, I., Boudaya, S., Ben Abdallah, F., Turki, H., Attia, H., & Hentati, B. (2009). Antioxidant enzymes and lipid peroxidation at the tissue level in patients with stable and active vitiligo. *International Journal of Dermatology*, *48*(5), 476–480. https://doi.org/10.1111/j.1365-4632.2009.03998.x
17. Esmat, S. M., Hadidi, H. H. E., Hegazy, R. A., Gawdat, H. I., Tawdy, A. M., Fawzy, M. M., AbdelHalim, D. M., Sultan, O. S., & Shaker, O. G. (2018). Increased tenascin C and DKK1 in vitiligo: possible role of fibroblasts in acral and non-acral disease. *Archives of Dermatological Research*, *310*(5), 425–430. https://doi.org/10.1007/s00403-018-1830-z
18. Ezzedine, K., Lim, H. W., Suzuki, T., Katayama, I., Hamzavi, I., Lan, C. C. E., Goh, B. K., Anbar, T., Silva de Castro, C., Lee, A. Y., Parsad, D., Van Geel, N., Le Poole, I. C., Oiso, N., Benzekri, L., Spritz, R., Gauthier, Y., Hann, S. K., Picardo, M., & Taieb, A. (2012). Revised classification/nomenclature of vitiligo and related issues: The Vitiligo Global Issues Consensus Conference. *Pigment Cell and Melanoma Research*, *25*(3). https://doi.org/10.1111/j.1755-148X.2012.00997.x
19. Gasque, P., & Jaffar-Bandjee, M. C. (2015). The immunology and inflammatory responses of human melanocytes in infectious diseases. In *Journal of Infection* (Vol. 71, Issue 4, pp. 413–421). W.B. Saunders Ltd. https://doi.org/10.1016/j.jinf.2015.06.006
20. Gauthier, Y., Cario-Andre, M., Lepreux, S., Pain, C., & Taïeb, A. (2003). Melanocyte detachment after skin friction in non lesional skin of patients with generalized vitiligo. *British Journal of Dermatology*, *148*, 95–101. https://academic.oup.com/bjd/article/148/1/95/6634562
21. Grace, M. A., Dias, L. A., Maze-Foley, K., Sinclair, C., Mullin, K. D., Garrison, L.,

doi:10.6342/NTU202302888

& Noble, L. (2018). Cookiecutter shark bite wounds on cetaceans of the Gulf of Mexico. In *Aquatic Mammals* (Vol. 44, Issue 5, pp. 491–499). European Association for Aquatic Mammals. https://doi.org/10.1578/AM.44.5.2018.491

22. Hartman, K. L., Visser, F., & Hendriks, A. J. E. (2008). Social structure of Risso's dolphins (Grampus griseus) at the Azores: A stratified community based on highly associated social units. *Canadian Journal of Zoology*, *86*(4), 294–306. https://doi.org/10.1139/Z07-138
23. Hartman, K. L., Wittich, A., Cai, J. J., Van Der Meulen, F. H., & Azevedo, J. M. N. (2016). Estimating the age of Risso's dolphins (Grampus griseus) based on skin appearance. *Journal of Mammalogy*, *97*(2), 490–502. https://doi.org/10.1093/jmammal/gyv193
24. Hashimoto, O., Ohtsuki, H., Kakizaki, T., Amou, K., Sato, R., Doi, S., Kobayashi, S., Matsuda, A., Sugiyama, M., Funaba, M., Matsuishi, T., Terasawa, F., Shindo, J., & Endo, H. (2015). Brown adipose tissue in cetacean blubber. *PLoS ONE*, *10*(2). https://doi.org/10.1371/journal.pone.0116734
25. Heath, R. L., Thomlinson, A. M., & Shah, M. (2009). Melanocytes and burn wound healing. *Burns*, *35*, S44. https://doi.org/10.1016/j.burns.2009.06.175
26. Iverson, S. J. (1985). The antitropical factor in cetacean speciation. In *Evolution* (Vol. 17, pp. 107–116). Blackwell Scientifi c Publications. http://www.seamap.env.
27. Jennifer Y. Lin, & David E. Fisher. (2007). Melanocyte biology and skin pigmentation. In *Nature* (Vol. 445, Issue 7130, pp. 843–850). Nature Publishing Group. https://doi.org/10.1038/nature05660
28. Keswell, D., Davids, L. M., & Kidson, S. H. (2012). DKK1 is highly expressed in the dermis of vitiligo lesion: Is there association between DKK1 and vitiligo? In *Journal of Dermatological Science* (Vol. 66, Issue 2, pp. 160–163). https://doi.org/10.1016/j.jdermsci.2012.01.005
29. L J. Bruce-Allen, & J. R. Geraci. (1987). Slow Process of Wound Repair in Beluga Whales, Delphinapterus leucas. *Canadian Journal of Fisheries and Aquatic Sciences*, *44*(9), 1661–1665.
30. MacLeod, C. D. (1998). Intraspecific scarring in odontocete cetaceans: an indicator of male 'quality' in aggressive social interactions? Journal of Zoology, 244(1), 71-77.
31. Maglietta, R., Renò, V., Cipriano, G., Fanizza, C., Milella, A., Stella, E., & Carlucci, R. (2018). DolFin: an innovative digital platform for studying Risso's dolphins in the Northern Ionian Sea (North-eastern Central Mediterranean). *Scientific Reports*, *8*(1). https://doi.org/10.1038/s41598-018-35492-3
32. Mariani, M., Miragliuolo, A., Mussi, B., Russo, G. F., Ardizzone, G., & Pace, D. S. (2016). Analysis of the natural markings of Risso's dolphins (Grampus griseus) in

doi:10.6342/NTU202302888

the central Mediterranean Sea. *Journal of Mammalogy*, *97*(6), 1512–1524. https://doi.org/10.1093/jmammal/gyw109

33. Martinez-Levasseur, L. M., Birch-Machin, M. A., Bowman, A., Gendron, D., Weatherhead, E., Knell, R. J., & Acevedo-Whitehouse, K. (2013). Whales Use Distinct Strategies to Counteract Solar Ultraviolet Radiation. *Scientific Reports*, *3*. https://doi.org/10.1038/srep02386
34. Martinez-Levasseur, L. M., Gendron, D., Knell, R. J., O'Toole, E. A., Singh, M., & Acevedo-Whitehouse, K. (2011). Acute sun damage and photoprotective responses in whales. *Proceedings of the Royal Society B: Biological Sciences*, *278*(1711), 1581–1586. https://doi.org/10.1098/rspb.2010.1903
35. Melissa J. Joblon, Mark A. Pokras, Brendan Morse, Charles T. Harry, Kathryn S. Rose, Sarah M. Sharp, Misty E. Niemeyer, Kristen M. Patchett, W. Brian Sharp, & Michael J. Moore. (2014). Body Condition Scoring System for Delphinids Based on Short-beaked Common Dolphins (*Delphinus delphis*). *Journal of Marine Animals and Their Ecology*, *7*, 5–13.
36. Menon, G. K. (2002). New insights into skin structure: scratching the surface. In *Advanced Drug Delivery Reviews* (Vol. 54). www.elsevier.com/locate/drugdeliv
37. Morales-Guerrero, B., Barragán-Vargas, C., Silva-Rosales, G. R., Ortega-Ortiz, C. D., Gendron, D., Martinez-Levasseur, L. M., & Acevedo-Whitehouse, K. (2017). Melanin granules melanophages and a fully-melanized epidermis are common traits of odontocete and mysticete cetaceans. *Veterinary Dermatology*, *28*(2), 213-e50. https://doi.org/10.1111/vde.12392
38. Park, H. Y., Kosmadaki, M., Yaar, M., & Gilchrest, B. A. (2009). Cellular mechanisms regulating human melanogenesis. In *Cellular and Molecular Life Sciences* (Vol. 66, Issue 9, pp. 1493–1506). https://doi.org/10.1007/s00018-009-8703-8
39. Rani, S., Chauhan, R., Parsad, D., & Kumar, R. (2018). Effect of Dickkopf1 on the senescence of melanocytes: in vitro study. *Archives of Dermatological Research*, *310*(4), 343–350. https://doi.org/10.1007/s00403-018-1820-1
40. Rastogi, R. P., Richa, Kumar, A., Tyagi, M. B., & Sinha, R. P. (2010). Molecular mechanisms of ultraviolet radiation-induced DNA damage and repair. In *Journal of Nucleic Acids* (Vol. 2010). https://doi.org/10.4061/2010/592980
41. Reeb, D., Best, P. B., & Kidson, S. H. (2007). Structure of the integument of southern right whales, *Eubalaena australis*. *Anatomical Record*, *290*(6), 596–613. https://doi.org/10.1002/ar.20535
42. Serre, C., Busuttil, V., & Botto, J. M. (2018). Intrinsic and extrinsic regulation of human skin melanogenesis and pigmentation. In *International Journal of Cosmetic Science* (Vol. 40, Issue 4, pp. 328–347). Blackwell Publishing Ltd.

doi:10.6342/NTU202302888

https://doi.org/10.1111/ics.12466
43. Shah, M., Heath, R., & Chadwick, S. (2012). Abnormal pigmentation within cutaneous scars: A complication of wound healing. In *Indian Journal of Plastic Surgery* (Vol. 45, Issue 2, pp. 403–411). https://doi.org/10.4103/0970-0358.101328
44. Shruti Dutta, Sangita Panda, Prashant Singh, Sumit Tawde, Mamata Mishra, Vikas Andhale, Angira Athavale, & Sunil Manohar Keswan. (2020). Hypopigmentation in burns is associated with alterations in the architecture of the skin and the dendricity of the melanocytes. *Burns*, *46*(4), 906–917. https://doi.org/10.1016/j.burns.2019.10.003
45. Snell, R. S. (1963). A study of the melanocytes and melanin in a healing deep wound. In *J. Anat. Lond* (Vol. 97, Issue 2).
46. Struntz, D. J., McLellan, W. A., Dillaman, R. M., Blum, J. E., Kucklick, J. R., & Pabst, D. A. (2004). Blubber Development in Bottlenose Dolphins (Tursiops truncatus). *Journal of Morphology*, *259*(1), 7–20. https://doi.org/10.1002/jmor.10154
47. Su, C. Y., Hughes, M. W., Liu, T. Y., Chuong, C. M., Wang, H. V., & Yang, W. C. (2022a). Defining Wound Healing Progression in Cetacean Skin: Characteristics of Full-Thickness Wound Healing in Fraser's Dolphins (Lagenodelphis hosei). *Animals*, *12*(5). https://doi.org/10.3390/ani12050537
48. Su, C. Y., Liu, T. Y., Wang, H. V., & Yang, W. C. (2023). Histopathological Study on Collagen in Full-Thickness Wound Healing in Fraser's Dolphins (Lagenodelphis hosei). *Animals*, *13*(10). https://doi.org/10.3390/ani13101681
49. Su, C. Y., Wang, H. V., Hughes, M. W., Liu, T. Y., Chuong, C. M., & Yang, W. C. (2022b). Successful Repigmentation of Full-Thickness Wound Healing in Fraser's Dolphins (Lagenodelphis hosei). *Animals*, *12*(12). https://doi.org/10.3390/ani12121482
50. Travis, T. E., Ghassemi, P., Ramella-Roman, J. C., Prindeze, N. J., Paul, D. W., Moffatt, L. T., Jordan, M. H., & Shupp, J. W. (2015). A multimodal assessment of melanin and melanocyte activity in abnormally pigmented hypertrophic scar. *Journal of Burn Care and Research*, *36*(1), 77–86. https://doi.org/10.1097/BCR.0000000000000154
51. Wagner, R. Y., Luciani, F., Cario-André, M., Rubod, A., Petit, V., Benzekri, L., Ezzedine, K., Lepreux, S., Steingrimsson, E., Taieb, A., Gauthier, Y., Larue, L., & Delmas, V. (2015). Altered E-cadherin levels and distribution in melanocytes precede clinical manifestations of vitiligo. *Journal of Investigative Dermatology*, *135*(7), 1810–1819. https://doi.org/10.1038/jid.2015.25
52. Wainwright, D. K., Fish, F. E., Ingersoll, S., Williams, T. M., St Leger, J., Smits, A. J., & Lauder, G. V. (2019). How smooth is a dolphin? The ridged skin of

doi:10.6342/NTU202302888

odontocetes. *Biology Letters*, *15*(7). https://doi.org/10.1098/rsbl.2019.0103

53. Wang, Z., Wang, Y., Bradbury, N., Gonzales Bravo, C., Schnabl, B., & Di Nardo, A. (2020). Skin wound closure delay in metabolic syndrome correlates with SCF deficiency in keratinocytes. *Scientific Reports*, *10*(1). https://doi.org/10.1038/s41598-020-78244-y
54. Yamaguchi, Y., Itami, S., Watabe, H., Yasumoto, K. I., Abdel-Malek, Z. A., Kubo, T., Rouzaud, F., Tanemura, A., Yoshikawa, K., & Hearing, V. J. (2004). Mesenchymal-epithelial interactions in the skin: Increased expression of dickkopf1 by palmoplantar fibroblasts inhibits melanocyte growth and differentiation. *Journal of Cell Biology*, *165*(2), 275–285. https://doi.org/10.1083/jcb.200311122
55. Yamaguchi, Y., Passeron, T., Hoashi, T., Watabe, H., Rouzaud, F., Yasumoto, K., Hara, T., Tohyama, C., Katayama, I., Miki, T., & Hearing, V. J. (2008). Dickkopf 1 (DKK1) regulates skin pigmentation and thickness by affecting Wnt/ β-catenin signaling in keratinocytes. *The FASEB Journal*, *22*(4), 1009–1020. https://doi.org/10.1096/fj.07-9475com

doi:10.6342/NTU202302888

Table 1. Details of sampled Risso's dolphins.

Animal ID	Gender	Age	Body length (cm)	Body condition	Carcass condition
KH20201003	Female	Calf	190	Thin	Code 2
KH20220103-1	Male	Juvenile	205	Normal	Code 2
KH20220103-2	Female	Juvenile	214	Normal	Code 2
TN20220612	Male	Juvenile	251	Thin	Code 2-3
NT20221022	Female	Calf	173	Thin	Code 2

doi:10.6342/NTU202302888

Table 2. Melanocytes counting in normal skin.

Sample number	Skin color	Location	MC count (MCs/mm)
1	Dark	N1	12.73
2	Dark	N3	13.37
3	Dark	N5	13.47
4	Dark	N7	18.24
5	Dark-gray	N2	11.96
6	Dark-gray	N4	9.29
7	Light-gray	N6	6.43
8	Light-gray	N6	5.52
9	Light-gray	N8	5.93
10	Grayish-white	N9	2.87
11	Grayish-white	N9	1.92
12	White	N10	0.15
13	White	N10	0.52

doi:10.6342/NTU202302888

Table 3. Melanocytes counting in wounds

MC = melanocyte

Sample number	Skin condition	Location in wounds	Skin color	MC count (MCs/mm)
14	Early stage 3	Migrating tongue	White	4.02
		Unwounded skin	Light-gray	12.71
15	Early stage 3	Migrating tongue	White	1.52
		Unwounded skin	Light-gray	20.66
16	Late stage 3	Central white area	White	0
		Migrating lines	Light-gray	2.85
		Periphery area	White	4.59
		Unwounded skin	Dark-gray	8.79
17	Stage 4	Central white area	White	0
		Migrating lines	Dark	10.72
		Periphery area	Light-gray	9.59
		Unwounded skin	Dark	12.01
18	Stage 4	Central white area	White	0
		Migrating lines	Grayish white	3.35
		Periphery area	Grayish white	12.79
		Unwounded skin	Light-gray	13.62
19	Stage 4	Central white area	White	0
		Migrating lines	Grayish white	3.5
		Periphery area	Grayish white	4.13
		Unwounded skin	Light-gray	9.94
20	Stage 5	Central white area	White	0
		Migrating lines	Dark	12.3
		Periphery area	Light-gray	10.5
		Unwounded skin	Dark	17.8

doi:10.6342/NTU202302888

Table 4. Melanocytes and melanin granules in hypopigmented scars at various stages in different species.

+: Melanocyte presented, –: Absence of melanocytes, MT: migrating tongue

	Melanocytes	Melanin granules	Reference
Risso's early stage 3 MT	+	+	This study
Risso's late stage 3 MT	–	–	This study
Fraser's stage 3 MT	+	+	Su *et al*, 2022b
Human MT	–	–	Heath *et al*, 2009
Risso's stage 4	–	–	This study
Fraser's stage 4	+	+	Su *et al*, 2022b
Human young scar	–	–	Breathnach, 1960
Risso's stage 5	–	–	This study
Fraser's stage 5	+	+	Su *et al*, 2022b
Human mature scar	+	–	Carney *et al*, 2021
Duroc pig mature scar	+	–	Carney *et al*, 2021

doi:10.6342/NTU202302888

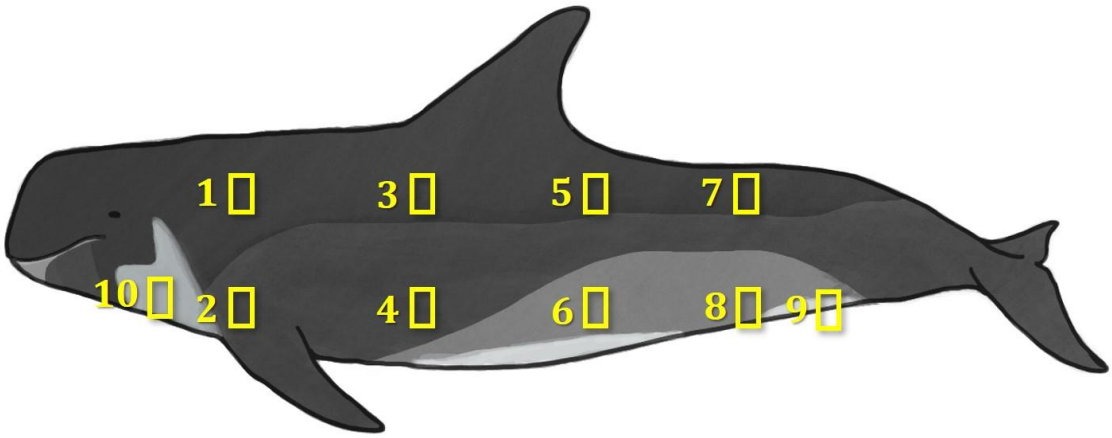

Figure 1. The sampling locations (N1-10) of Risso's dolphins in this study. Dark skin samples were collected from dorsal-lateral, dark-gray skin samples from lateral trunk, light-gray skin samples from peduncle, grayish withe samples from thorax and white skin samples from ventral side.

doi:10.6342/NTU202302888

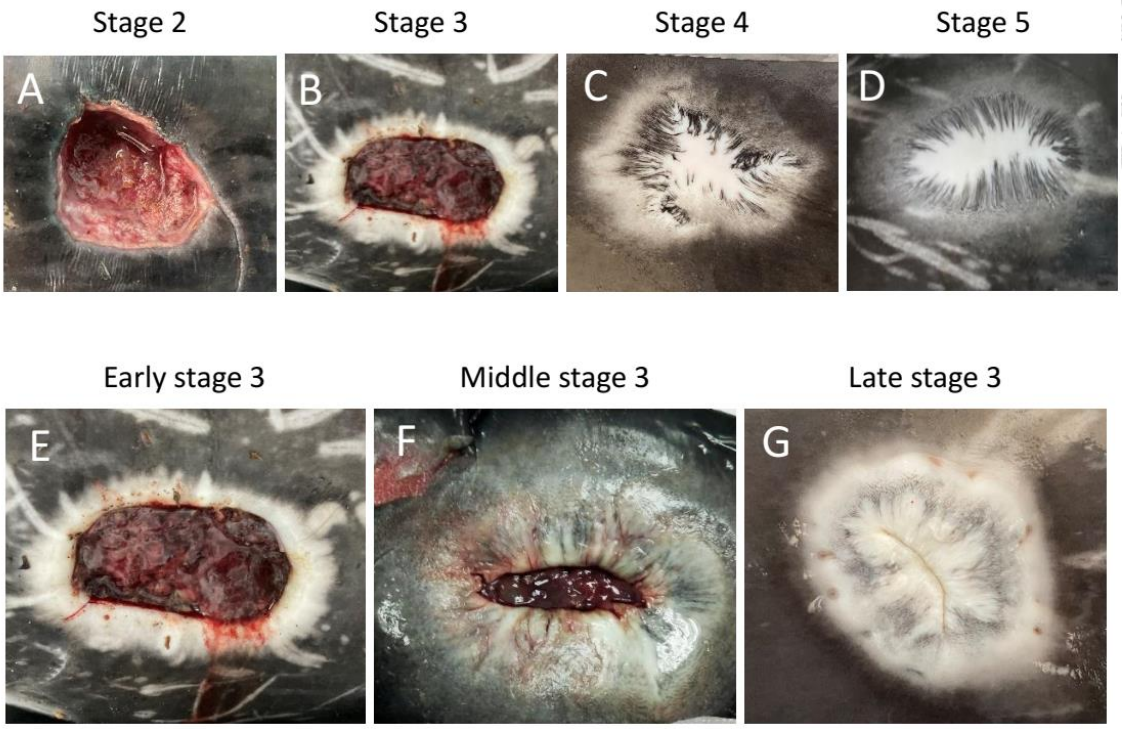

Figure 2. Gross appearance of white scars in each stage of wound healing. (A) Stage 2. (B) Stage 3. (C) Stage 4. (D) Stage 5. (E) Early stage 3. (F) Middle stage 3. (G) Late stage 3.

doi:10.6342/NTU202302888

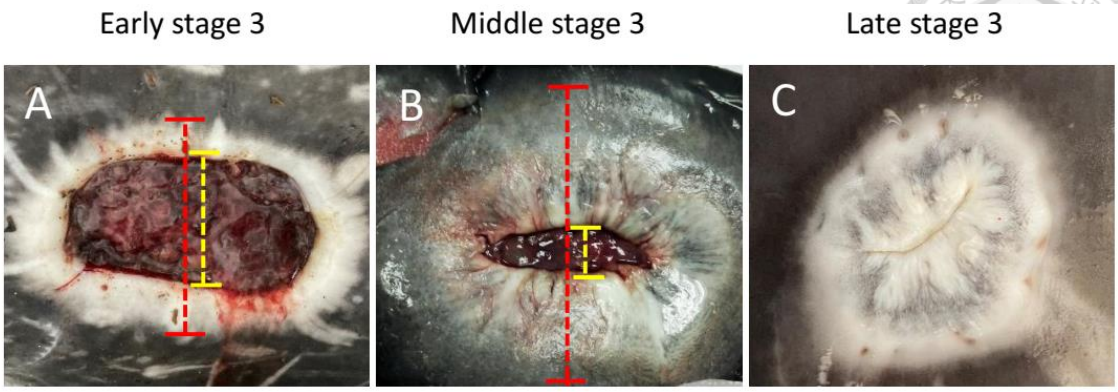

Figure 3. Distinguishing different stage 3 wounds. (A) The early stage 3 wound is defined as having a ratio greater than one- half between the diameter of the initial wound (red dashed line) and the minor axis of the incompletely epithelialized granulation tissue (yellow dashed line). (B) The middle stage 3 wound is defined by a ratio lower than one-half between the diameter of the initial wound (red dashed line) and the minor axis of the incompletely epithelialized granulation tissue (yellow dashed line). (C) The late stage 3 wound is defined as an incompletely epithelialized wound where granulation tissue is no longer visible to the naked eye.

doi:10.6342/NTU202302888

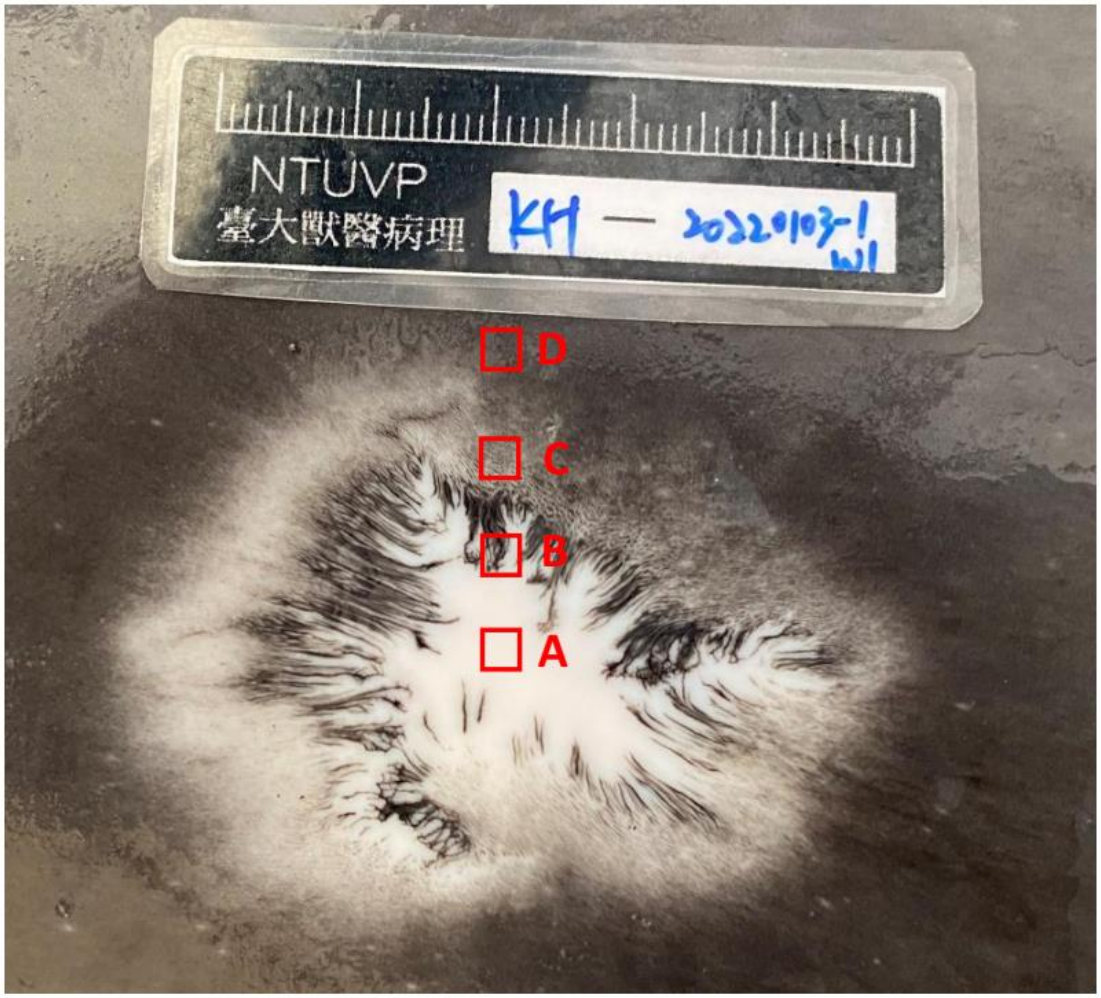

Figure 4. Gross appearance of white scars. (A) Central white area. (B) Migrating lines. (C) Periphery area. (D) Unwounded skin.

doi:10.6342/NTU202302888

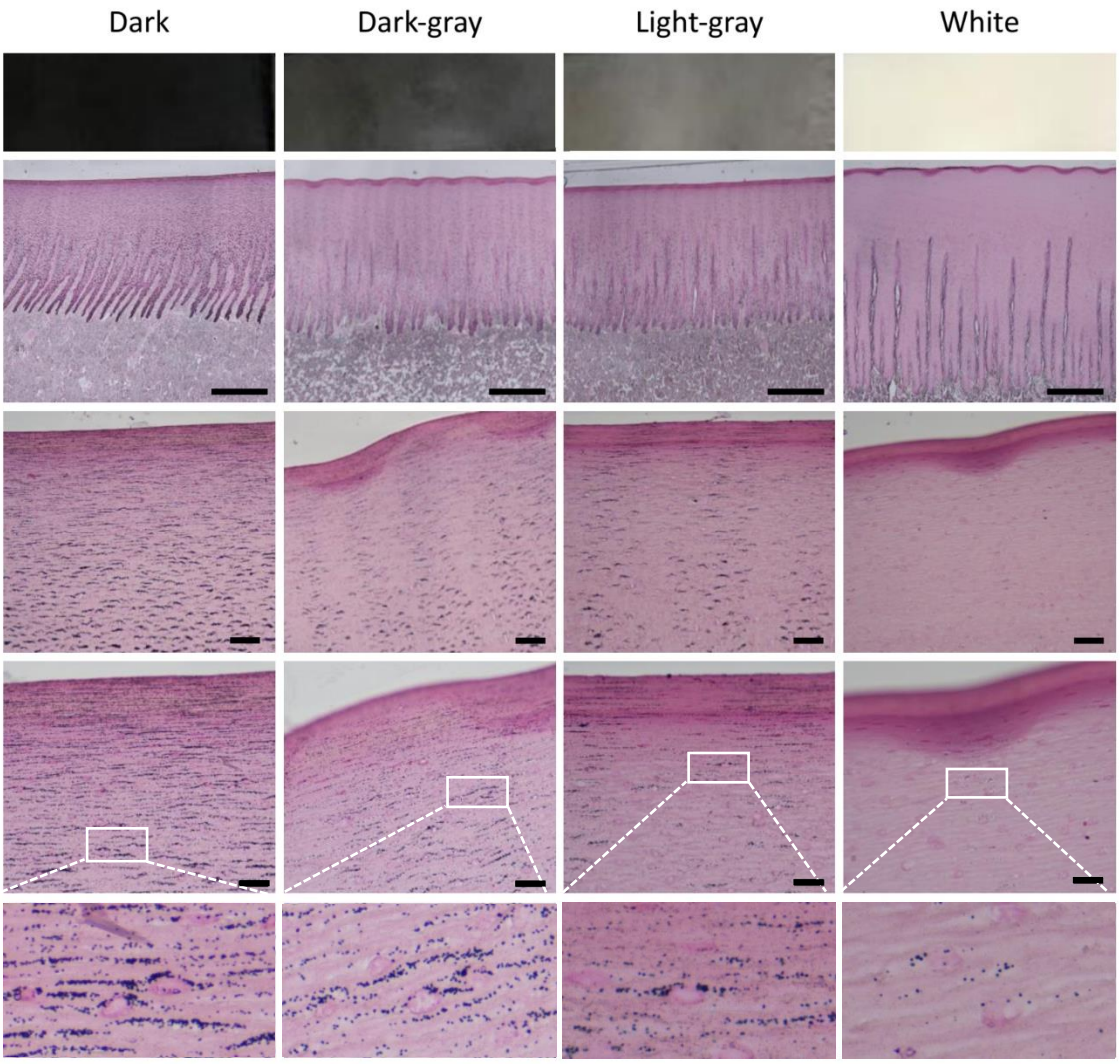

Figure 5. Fontana-Masson staining of dark, dark-gray, light-gray and white normal skin in Risso's dolphins. Melanin granules were distributed across the entire epidermal layer, extending to the outermost stratum even in white skin. A notable pattern of melanin granule accumulation directly above the keratinocyte nucleus was evident across all skin samples. The final row exhibits magnified images extracted from the demarcated area indicated by the white dotted frame. (scale bar = 500 μm in first role, 50 μm in second role and 25 μm in third role)

doi:10.6342/NTU202302888

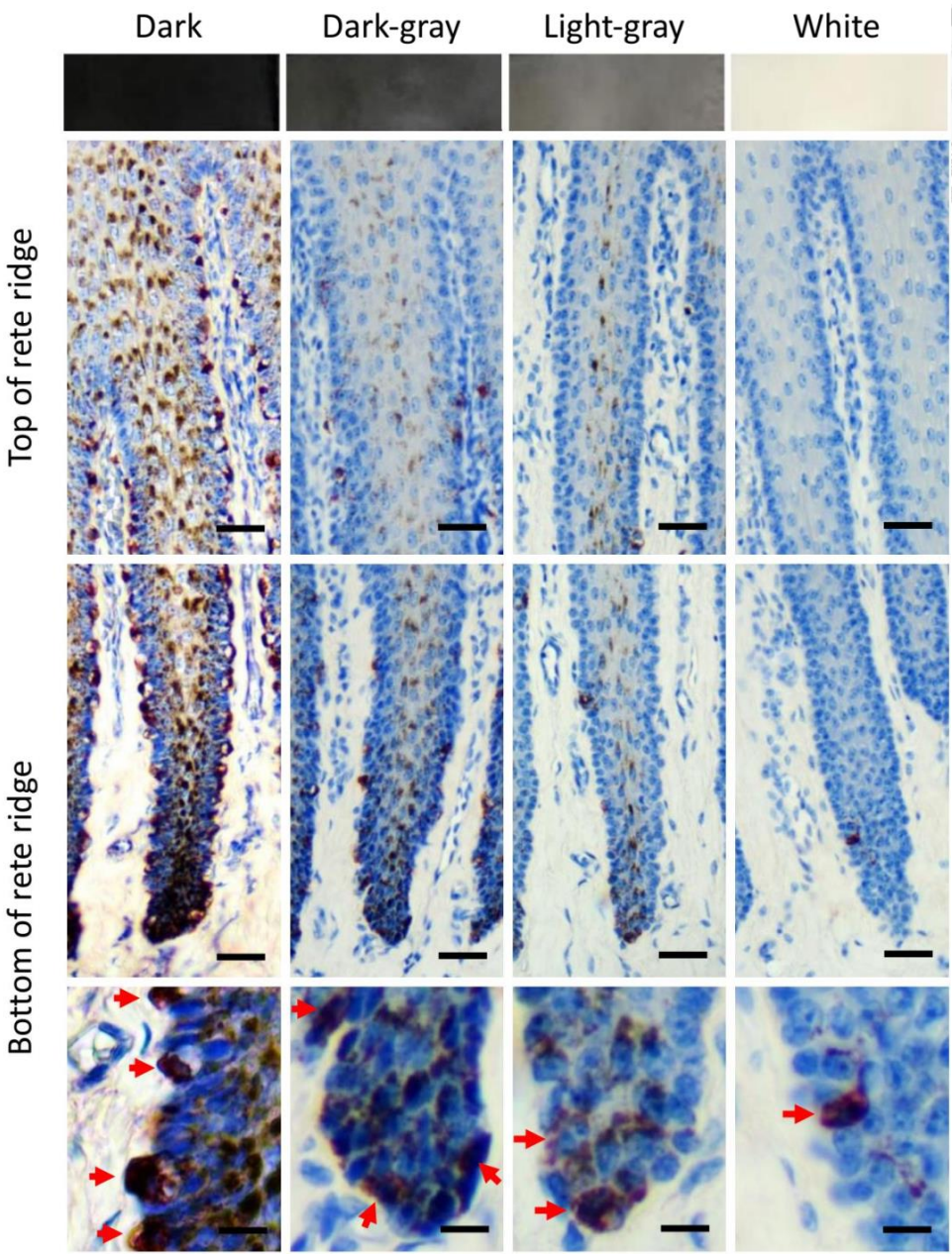

Figure 6. Immunohistochemical staining with cocktail antibody in dark, dark-gray, light-gray and white normal skin of Risso's dolphins. Melanocytes positively stained (arrow) were found in the basal layer. The darker the skin color, the greater the number of melanocytes, and melanocytes were mainly concentrated at the bottom of rete ridges. (Scale bar = 50 μm in top two role, 10 μm in last role).

doi:10.6342/NTU202302888

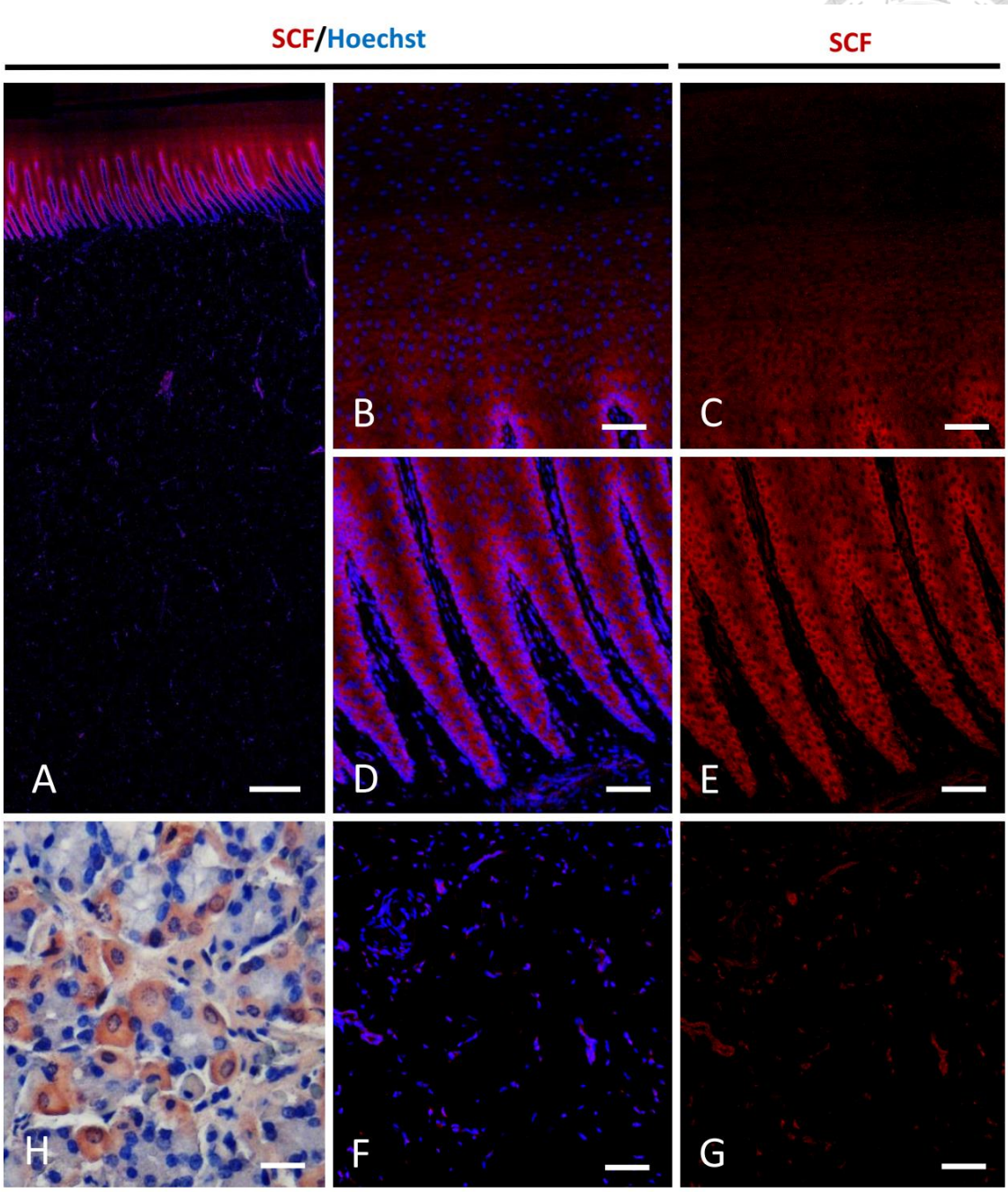

Figure 7. Immunofluorescence staining with SCF antibody in normal skin. (A) Low power view of normal light-gray skin (location=N8). (B-C) SCF expression in sternum spinosum. (D-E) SCF expression in rete ridge. (F-G) SCF expression in reticular dermis. (H) Positive control of SCF in intestine of Risso's dolphins, IHC staining. (scale bar = 500 μm in A, 25 μm in B-H)

doi:10.6342/NTU202302888

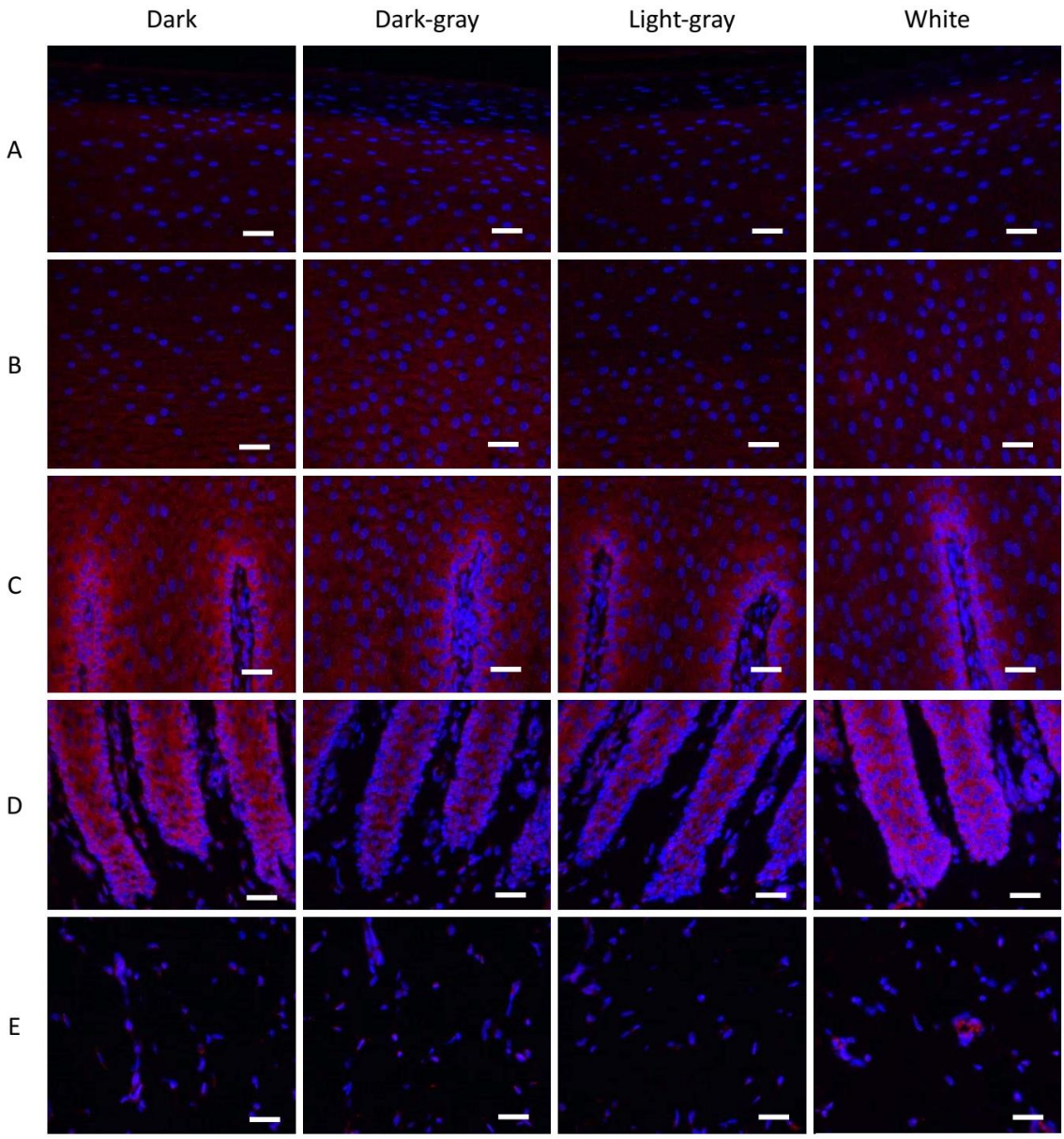

Figure 8. Immunofluorescence staining with SCF antibody in dark, dark-gray, light-gray and white normal skin of Risso's dolphins. (A) Stratum externum. (B) Stratum spinosum. (C) Top of rete ridge. (D) Bottom of rete ridge. (E) Reticular dermis. (Scale bar = 30 μm)

doi:10.6342/NTU202302888

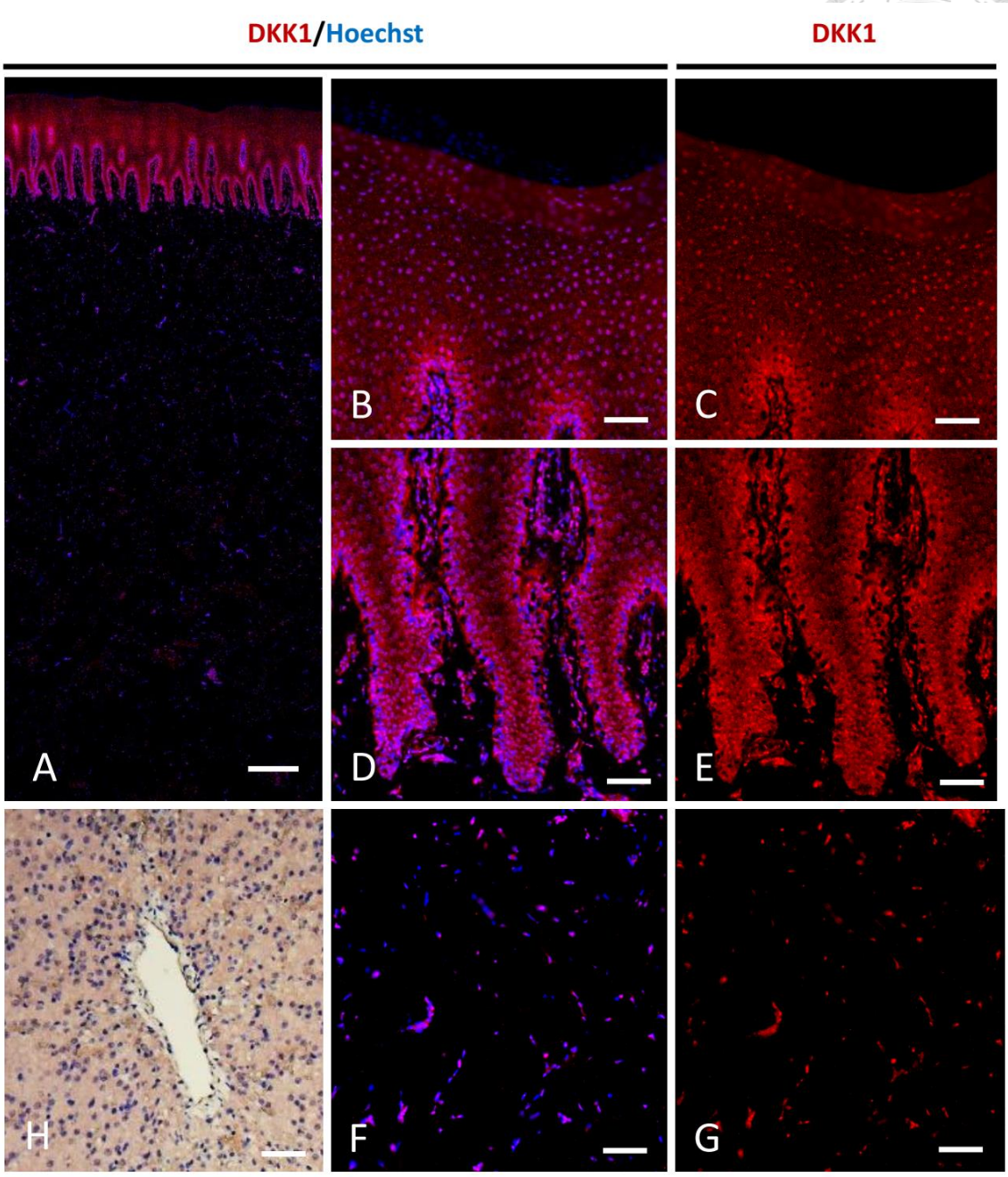

Figure 9. Immunofluorescence staining with DKK1 antibody in normal skin (A) Low power view of normal light-gray skin (location=N8). (B-C) DKK1 expression in stratum spinosum. (D-E) DKK1 expression in rete ridge. (F-G) DKK1 expression in reticular dermis. (H) Positive control of DKK1 in liver of Risso's dolphins, IHC staining. (Scale bar = 500 μm in A, 25 μm in F-G, 50 μm in H)

doi:10.6342/NTU202302888

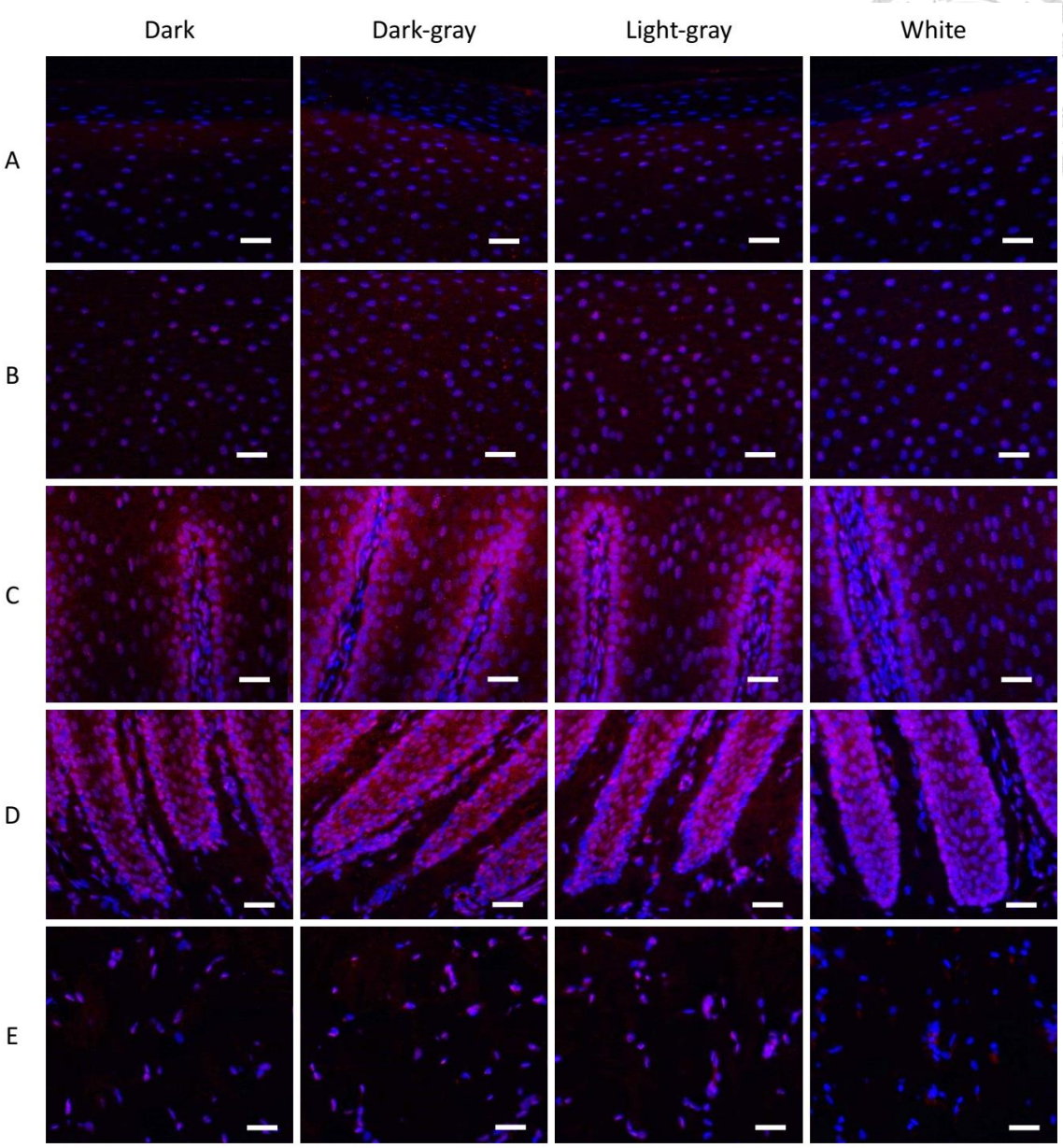

Figure 10. Immunofluorescence staining with DKK1 antibody in normal dark, dark-gray, light-gray, white normal skin of Risso's dolphins. (A) Stratum externum. (B) Stratum spinosum. (C) Top of rete ridge. (D) Bottom of rete ridge. (E)Reticular dermis. (Scale bar = 30 μm)

doi:10.6342/NTU202302888

Figure 11. Melanin distribution in an early stage 3 wound, Fontana-Masson staining. (A) The image presents a low-power view of an early stage 3 wound, where the migrating tongue is situated on the left side, and the right side portrays the normal dark gray skin. (B) In the rete ridge of migrating tongue, a small number of melanin granules could be observed. The upper right image illustrated a magnified view of the region from white dotted frame. (C) In the normal dark-gray skin adjacent to the wound, abundant melanin granules are evident throughout every layer of the epidermis. (Scale bar = 50 μm in last role)

doi:10.6342/NTU202302888

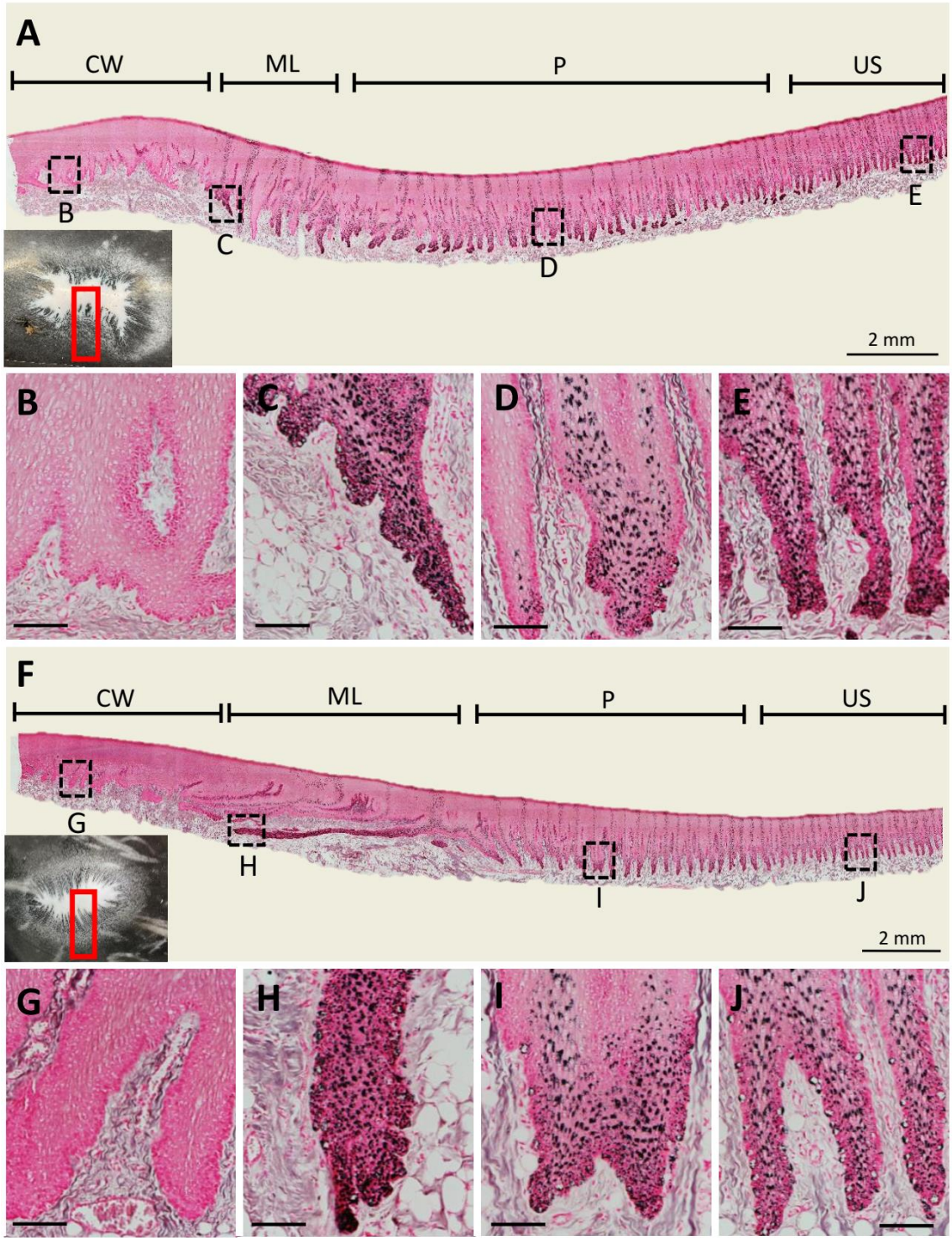

CW= Central white area, ML= Migrating lines, P=Periphery area, US=Unwounded skin.

doi:10.6342/NTU202302888

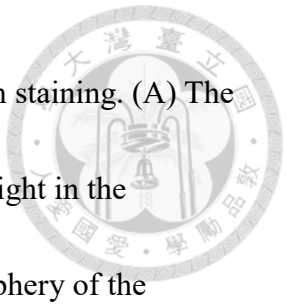

Figure 12. Melanin distribution in stage 4-5 wounds, Fontana-Masson staining. (A) The image presented a low-power view of a stage 4 wound. From left to right in the photograph, it represented the progression from the center to the periphery of the wound. (B) In the central white area of the stage 4 scar, the absence of melanin staining was observed throughout every layer of the epidermis. (C) The migrating lines area of the stage 4 scar exhibited a large amount of melanin granules throughout the epidermis. (D) In the periphery area of the stage 4 scar, melanin granules were observed throughout the epidermis. (E) Unwounded dark-gray skin. (F) The image presented a low-power view of a stage 5 wound. (G) In the central white area of the stage 5 scar, the absence of melanin staining was observed throughout every layer of the epidermis. (H) The migrating lines area of the stage 5 scar exhibited a large amount of melanin granules throughout the epidermis. (I) In the periphery area of the stage 5 scar, melanin granules were observed throughout the epidermis. (J) Unwounded dark skin. (Scale bar= 100 μm in B-E and G-J)

doi:10.6342/NTU202302888

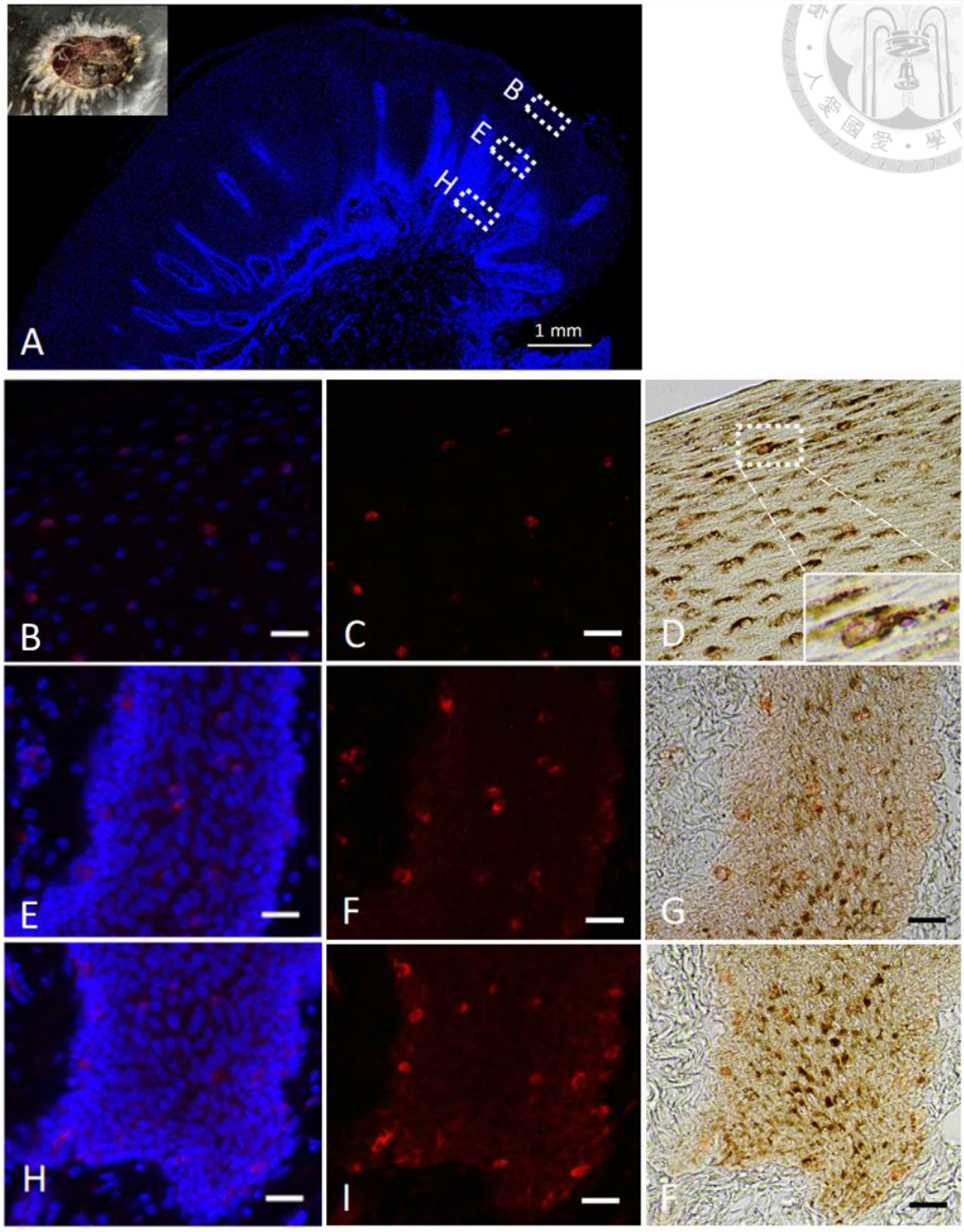

Figure 13. Melanocytes detachment in early stage 3 wound. (A) Low power view of migrating tongue in early stage 3 wound. (B-D) Stratum externum. (E-G) Middle of rete ridge. (H-F) Bottom of rete ridge. (Scale bar = 25 μm)

doi:10.6342/NTU202302888

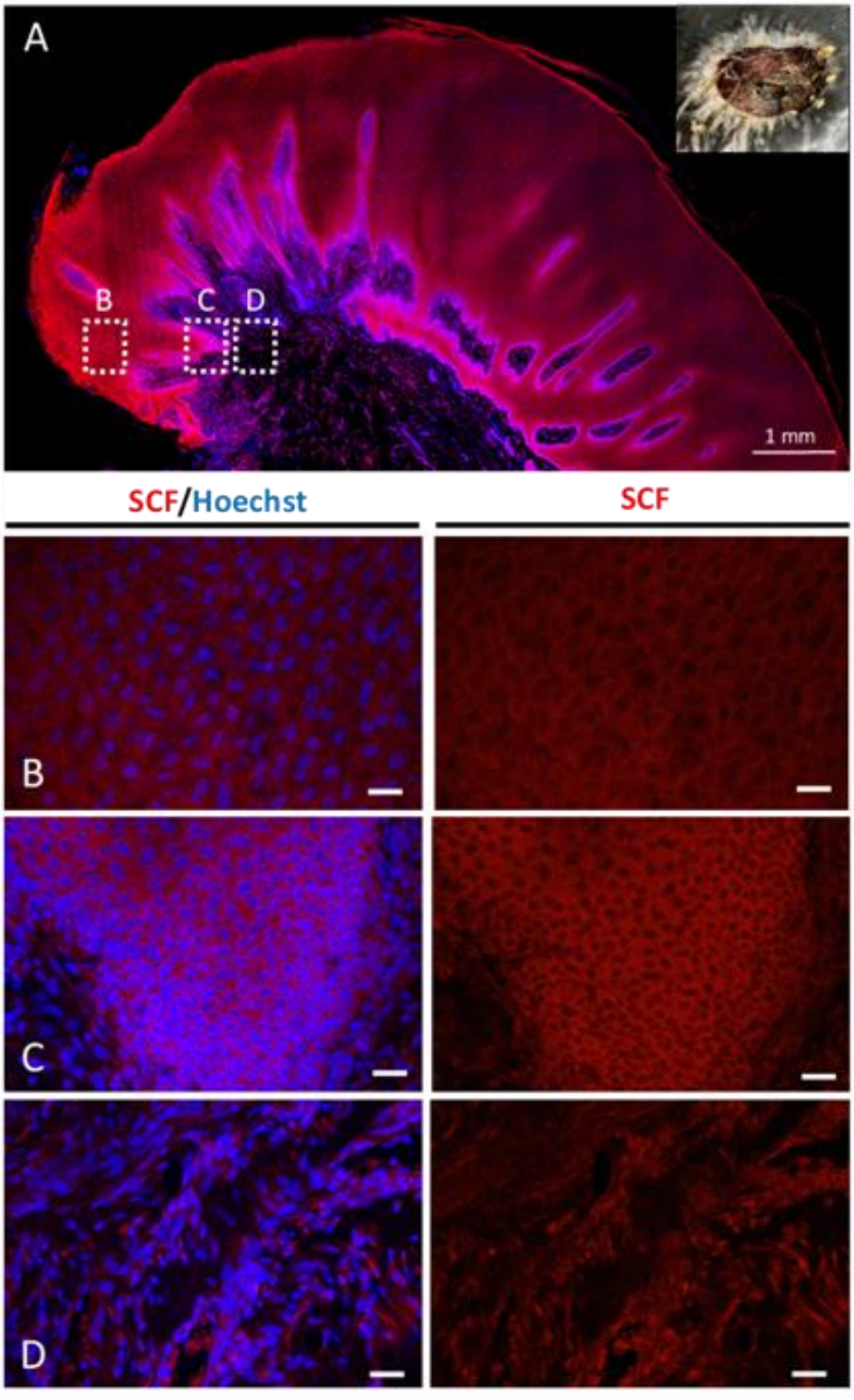

Figure 14. Immunofluorescence staining with SCF antibody in early stage 3 wounds. (A) Low power view of migrating tongue in early stage 3 wound. (B) Stratum spinosum. (C) Bottom of rete ridge. (D) Reticular dermis. (Scale bar = 25 μm)

doi:10.6342/NTU202302888

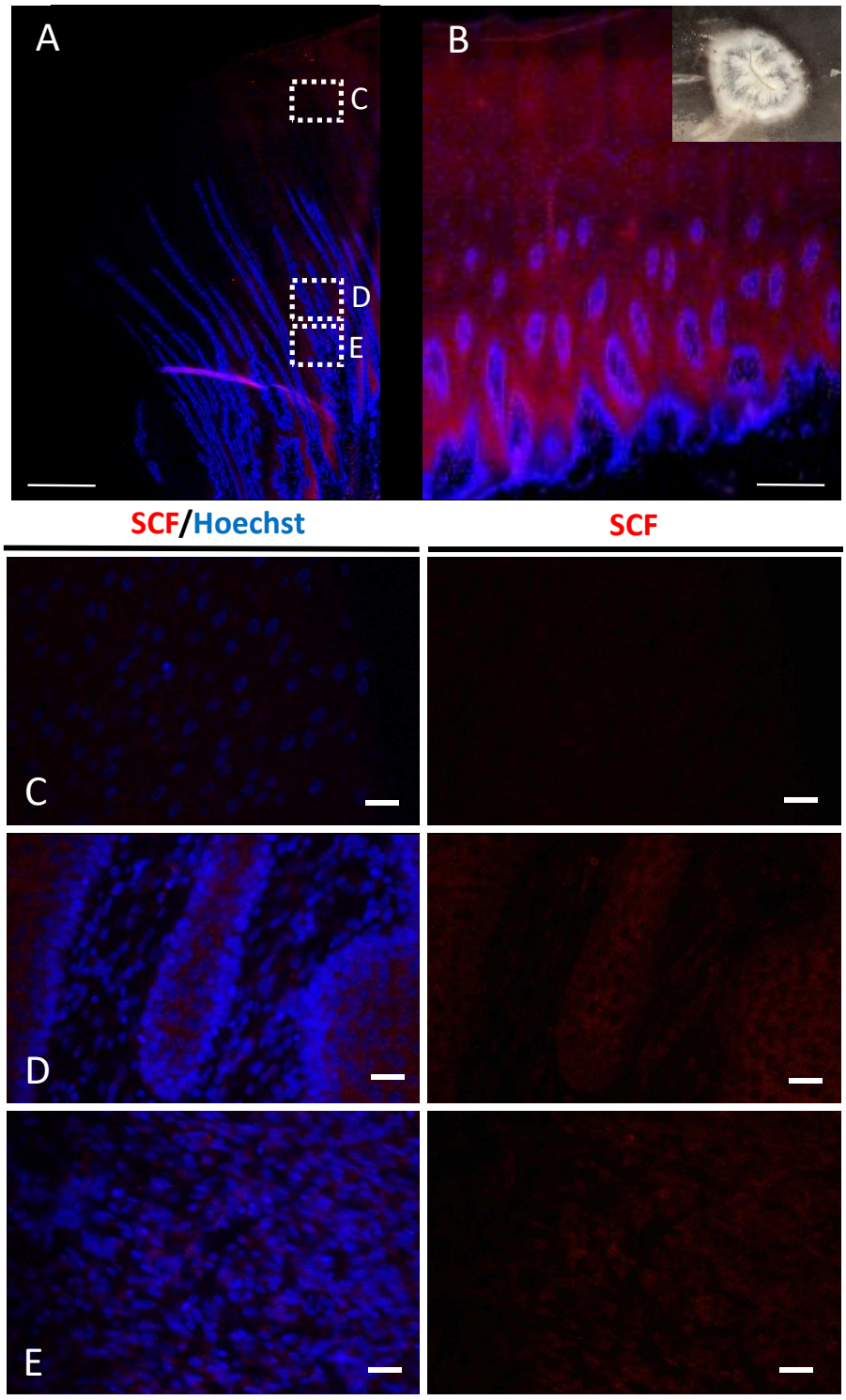

Figure 15. Immunofluorescence staining with SCF antibody in late stage 3 wounds. (A) Low power view of late stage 3 wound in migrating tongue. (B) Low power view of late stage 3 wound in periphery area. (C) Stratum spinosum. (D) Bottom of rete ridge. (E) Reticular dermis. (Scale bar = 25 μm)

doi:10.6342/NTU202302888

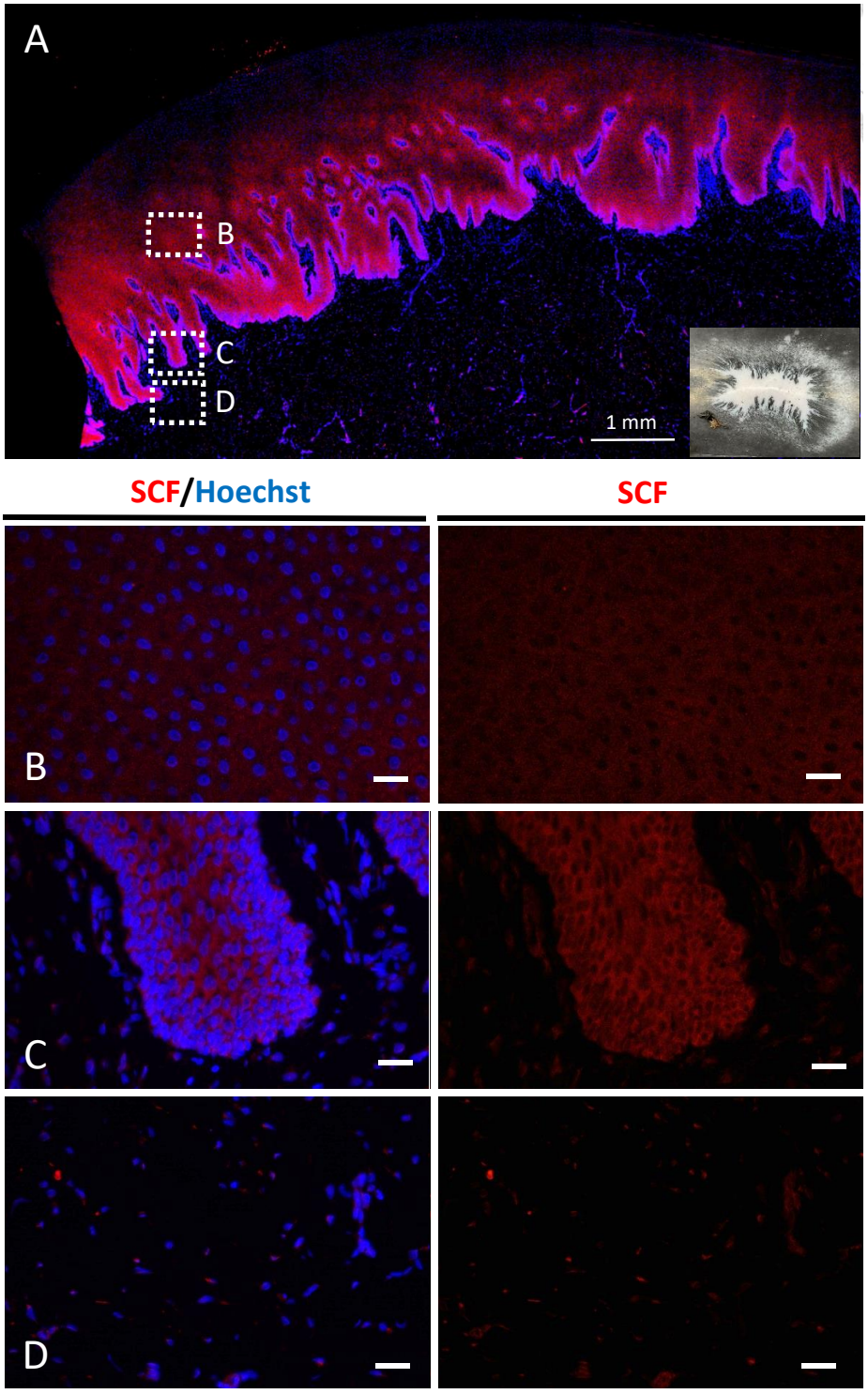

Figure 16. Immunofluorescence staining with SCF antibody in stage 4 wounds. (A) Low power view of stage 4 wound in central white area. (B) Stratum spinosum. (C) Bottom of rete ridge. (D) Reticular dermis. (Scale bar = 25 μm)

doi:10.6342/NTU202302888

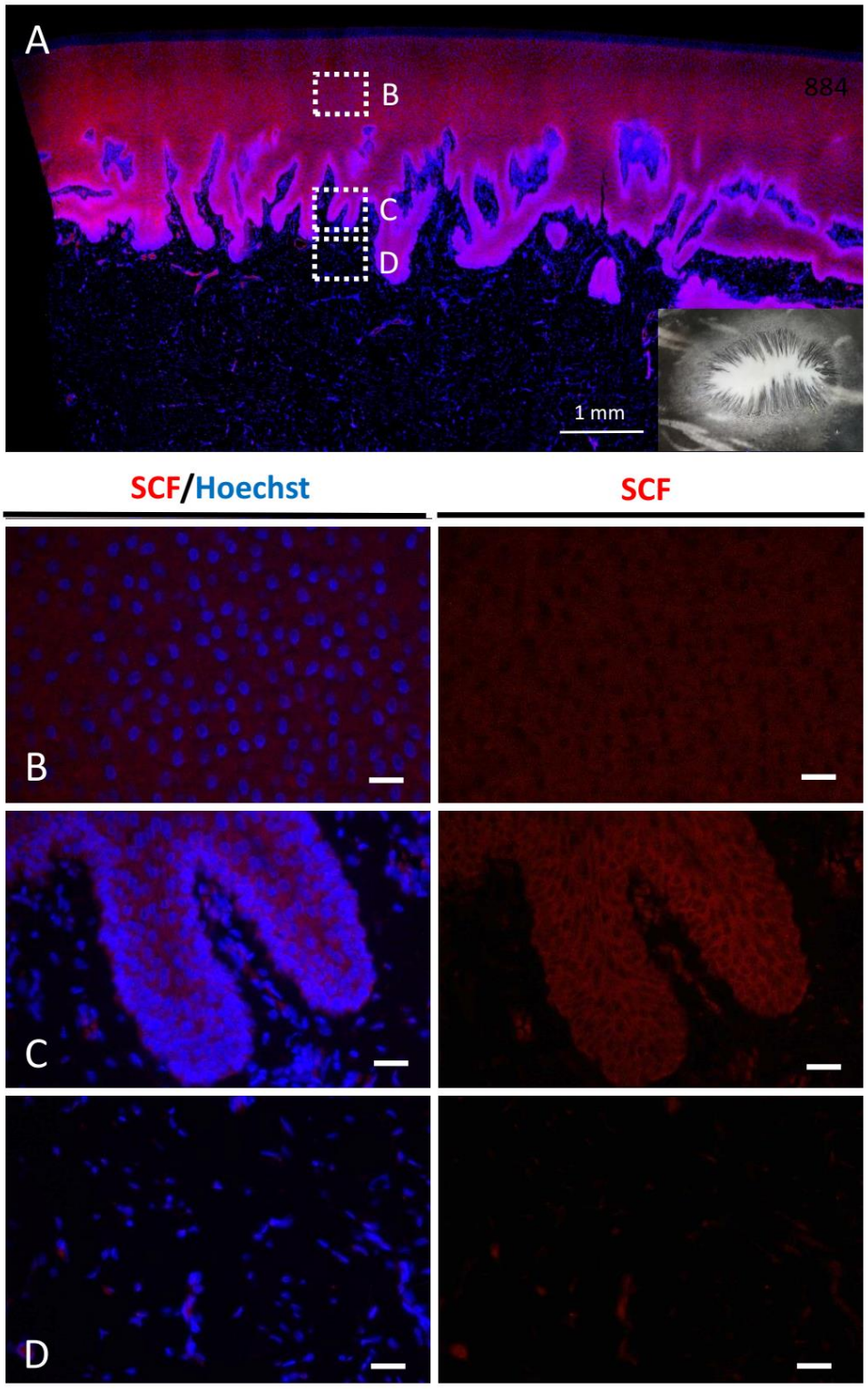

Figure 17. Immunofluorescence staining with SCF antibody in stage 5 wounds.

(A) Low power view of stage 5 wound in central white area. (B) Stratum spinosum. (C) Bottom of rete ridge. (D) Reticular dermis. (Scale bar = 25 μm)

doi:10.6342/NTU202302888

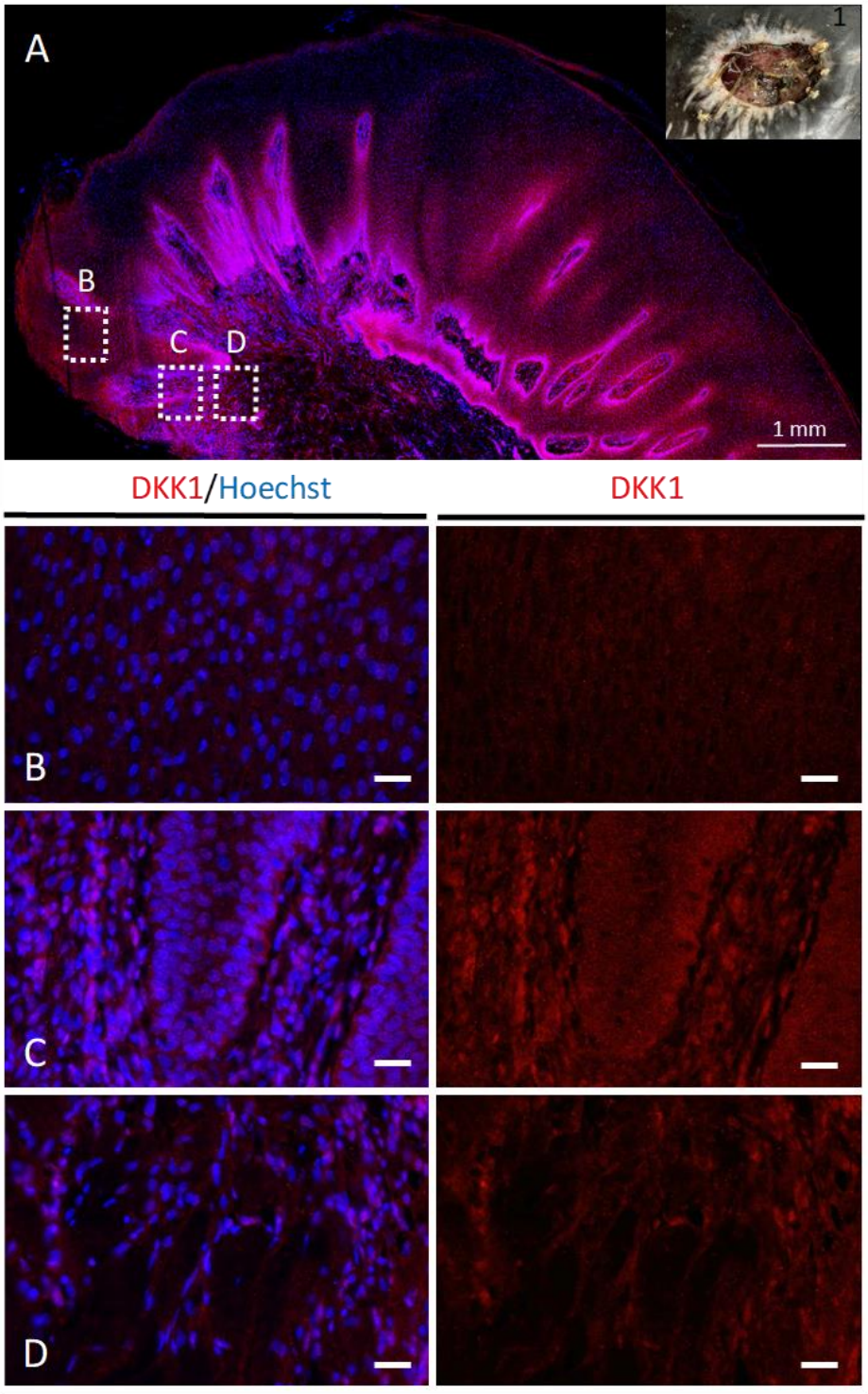

Figure 18. Immunofluorescence staining with DKK1 antibody in early stage 3 wounds. (A) Low power view of migrating tongue in early stage 3 wound. (B) Stratum spinosum. (C) Bottom of rete ridge. (D) Reticular dermis. (Scale bar = 25 μm)

doi:10.6342/NTU202302888

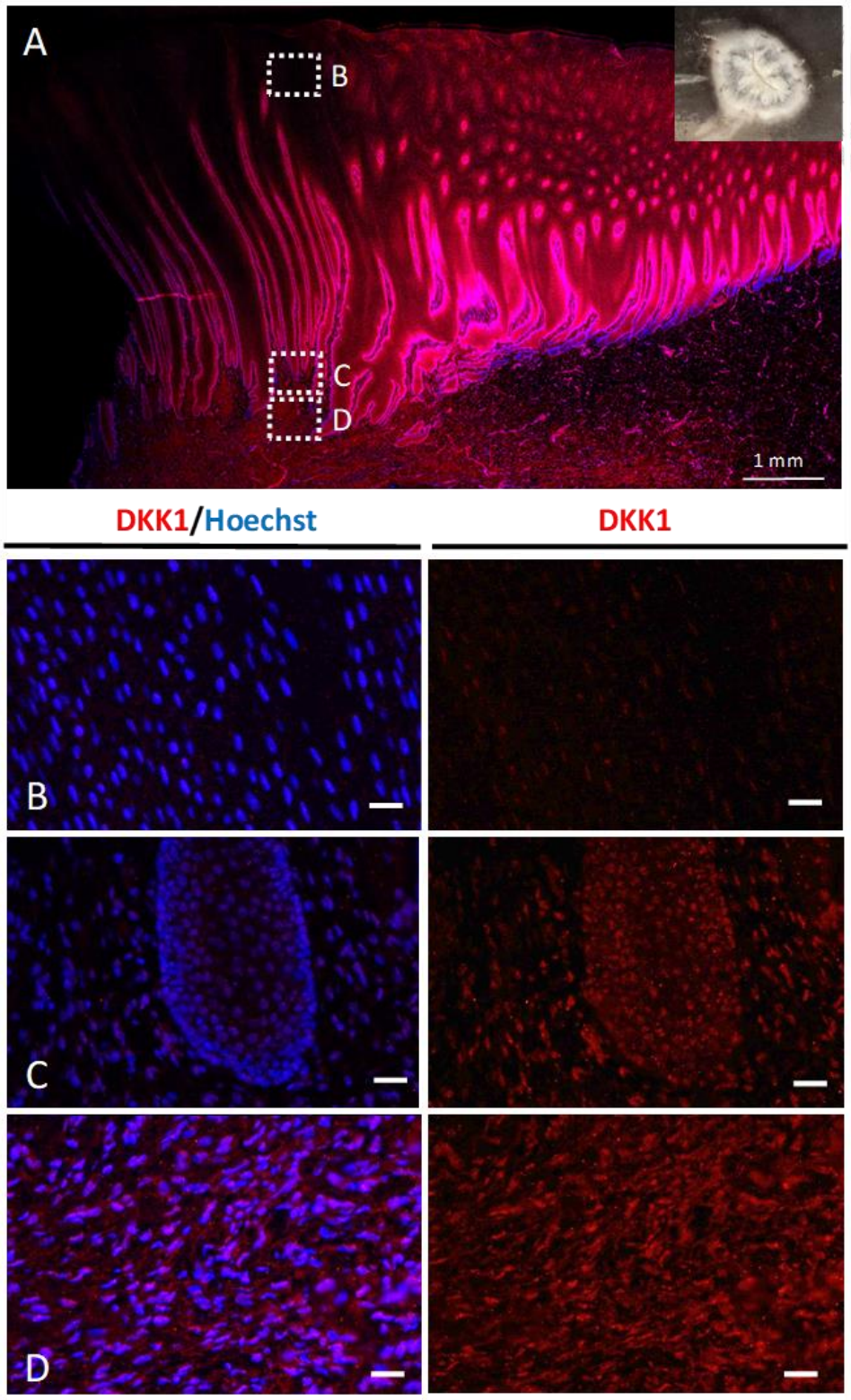

Figure 19. Immunofluorescence staining with DKK1 antibody in late stage 3 wounds.

(A) Low power view of migrating tongue in late stage 3 wound. (B) Stratum spinosum.

(C) Bottom of rete ridge. (D) Reticular dermis. (Scale bar = 25 μm)

doi:10.6342/NTU202302888

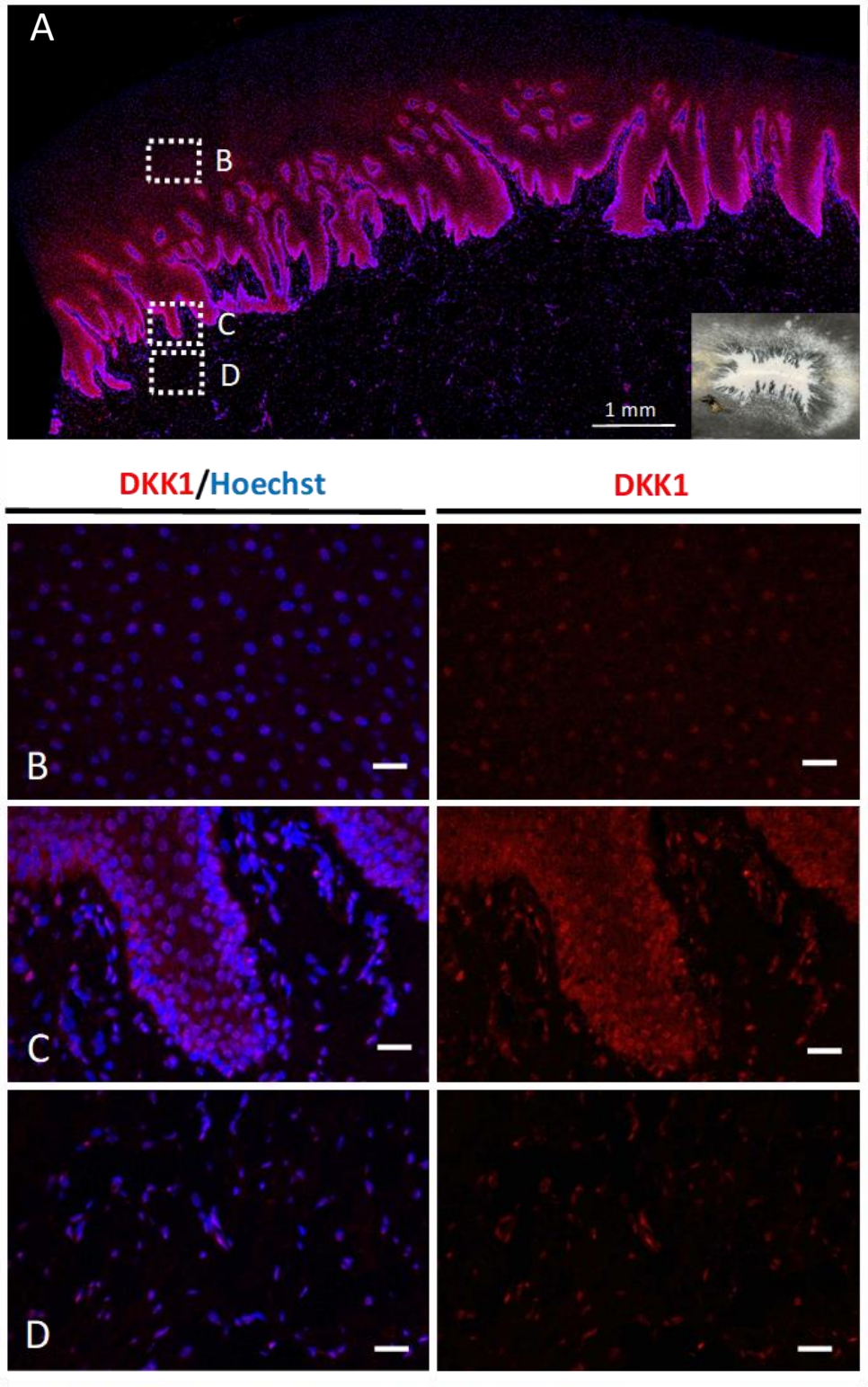

Figure 20. Immunofluorescence staining with DKK1 antibody in stage 4 wounds.

(A) Low power view of central white area in stage 4 wound. (B) Stratum spinosum. (C) Bottom of rete ridge. (D) Reticular dermis. (Scale bar = 25 μm)

doi:10.6342/NTU202302888

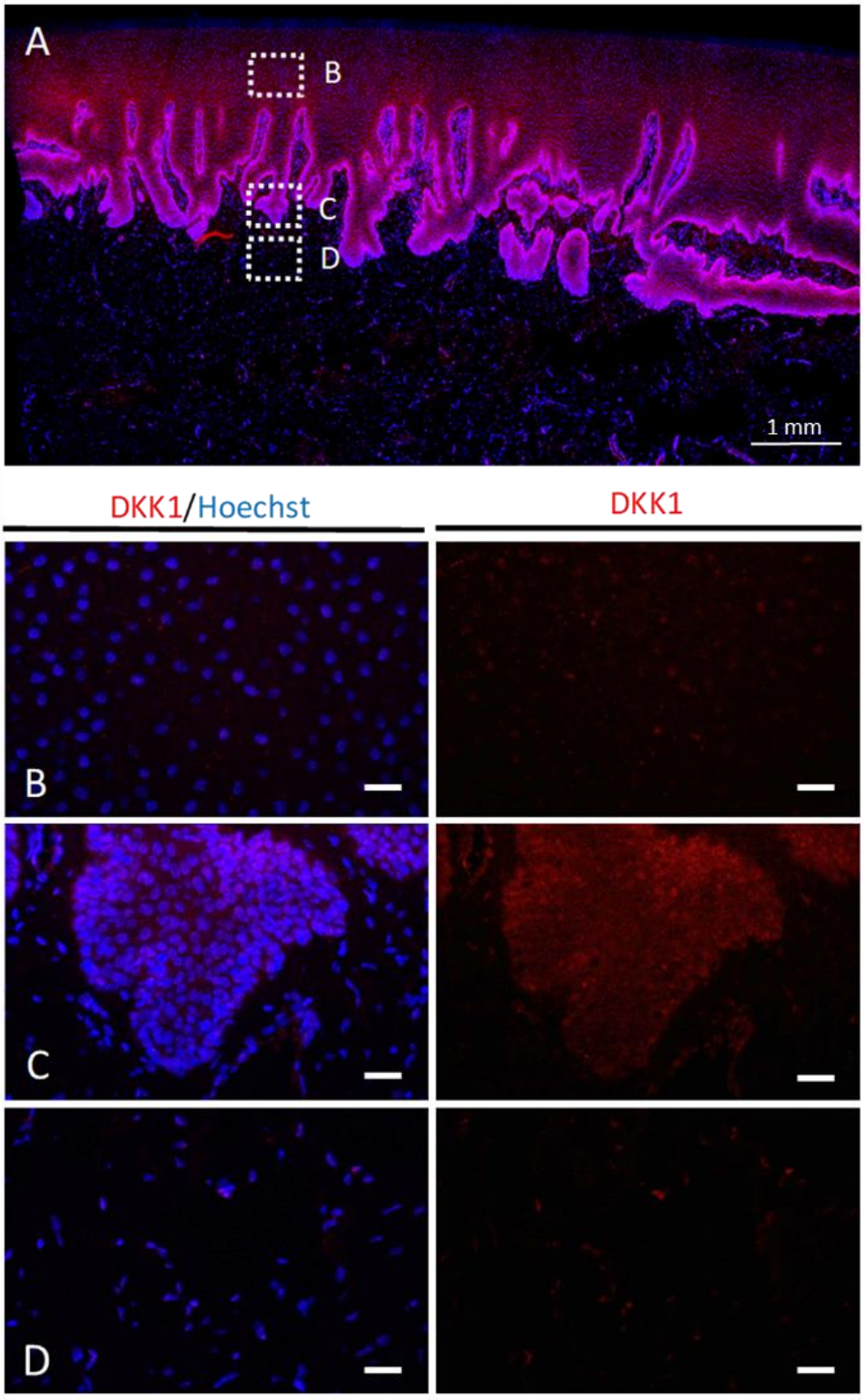

Figure 21. Immunofluorescence staining with DKK1 antibody in stage 5 wounds.

(A) Low power view of central white area in stage 5 wound. (B) Stratum spinosum. (C) Bottom of rete ridge. (D) Reticular dermis. (Scale bar = 25 μm)

doi:10.6342/NTU202302888

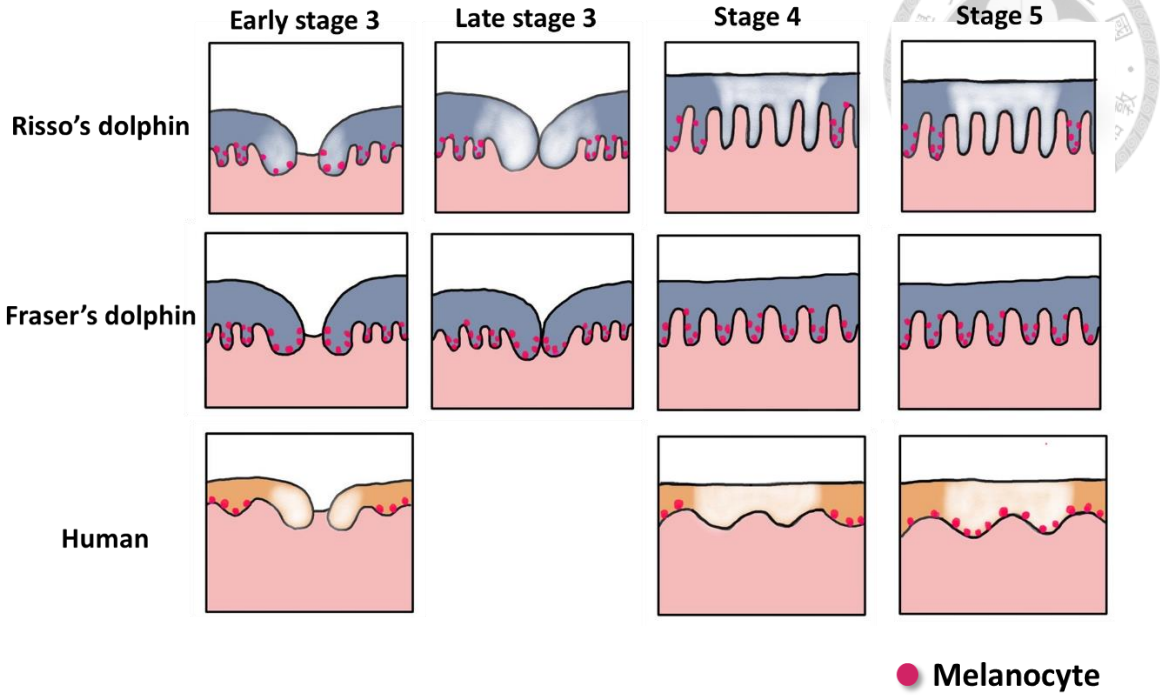

Figure 22. Summary diagram of melanocytes in hypopigmented scars at various stages in different species.

doi:10.6342/NTU202302888